Dual neutralization of influenza virus hemagglutinin and neuraminidase by a bispecific antibody leads to improved antiviral activity

Romila Moirangthem, Sapir Cordela, Dina Khateeb, Ben Shor, Ivan Kosik, Dina Schneidman-Duhovny, Michal Mandelboim, Friederike Jönsson, Jonathan Yewdell, Timothée Bruel, et al.

Molecular Therapy
Original Article

Dual neutralization of influenza virus hemagglutinin and neuraminidase by a bispecific antibody leads to improved antiviral activity

Romila Moirangthem,[1] Sapir Cordela,[1] Dina Khateeb,[1] Ben Shor,[2] Ivan Kosik,[3] Dina Schneidman-Duhovny,[2] Michal Mandelboim,[4] Friederike Jönsson,[5,6] Jonathan W. Yewdell,[3] Timothée Bruel,[7,8] and Yotam Bar-On[1]

[1]Department of Immunology, Rappaport Faculty of Medicine, Technion-Israel Institute of Technology, Haifa 3525422, Israel; [2]School of Computer Science and Engineering, The Hebrew University of Jerusalem, Jerusalem 9190501, Israel; [3]Cellular Biology Section, Laboratory of Viral Diseases, NIAID, Bethesda, MD 20892, USA; [4]Central Virology Laboratory, Sheba Medical Center, Tel Hashomer 52621, Israel; [5]Institut Pasteur, Université de Paris, Unit of Antibodies in Therapy and Pathology; Inserm UMR1222, Paris 75015, France; [6]CNRS, Paris 75015, France; [7]Virus and Immunity Unit, Institut Pasteur, Université Paris Cité; CNRS UMR3569, Paris, France; [8]Vaccine Research Institute, Créteil, France

Targeting multiple viral proteins is pivotal for sustained suppression of highly mutable viruses. In recent years, broadly neutralizing antibodies that target the influenza virus hemagglutinin and neuraminidase glycoproteins have been developed, and antibody monotherapy has been tested in preclinical and clinical studies to treat or prevent influenza virus infection. However, the impact of dual neutralization of the hemagglutinin and neuraminidase on the course of infection, as well as its therapeutic potential, has not been thoroughly tested. For this purpose, we generated a bispecific antibody that neutralizes both the hemagglutinin and the neuraminidase of influenza viruses. We demonstrated that this bispecific antibody has a dual-antiviral activity as it blocks infection and prevents the release of progeny viruses from the infected cells. We show that dual neutralization of the hemagglutinin and the neuraminidase by a bispecific antibody is advantageous over monoclonal antibody combination as it resulted an improved neutralization capacity and augmented the antibody effector functions. Notably, the bispecific antibody showed enhanced antiviral activity in influenza virus-infected mice, reduced mice mortality, and limited the virus mutation profile upon antibody administration. Thus, dual neutralization of the hemagglutinin and neuraminidase could be effective in controlling influenza virus infection.

INTRODUCTION

Most human viral vaccines prevent infection because of their ability to elicit neutralizing antibodies that block virus entry.[1] However, highly mutable viruses such as influenza virus and HIV-1 pose a great challenge for vaccine development, as attempts to design a vaccine that will elicit neutralizing antibodies against all the circulating variants have yet to be successful.[2] As an alternative, broadly neutralizing antibodies (bNAbs) that are able to recognize and neutralize a large portion of the circulating viruses were developed, and passive immunization with bNAbs was shown to suppress influenza virus and HIV-1 replication in preclinical and human studies.[3–8] Nevertheless, since highly mutable viruses have shown the capacity to develop resistance to bNAbs during the course of antibody therapy,[6–8] passive immunization with a combination of bNAbs directed against different viral epitopes is currently being tested for its ability to better control these viruses.[9] This was also a leading therapeutic strategy during the COVID-19 pandemic.[10] Moreover, combination therapy has become a cornerstone of cancer treatment.[11]

Most of the bNAbs against influenza virus target the influenza virus surface glycoprotein hemagglutinin (HA),[12,13] which is responsible for binding of the virus to cells and for initiating the infection.[14] The HA possesses two domains: the head, which comprises the receptor-binding site (RBS) that binds sialic acids on the surface of the target cells, and the stem, which is responsible for fusion of the viral membrane and the cellular membrane.[15] BNAbs against the HA can both target the HA head and inhibit the attachment of the virus to the target cell or the HA stem and interfere with the viral fusion machinery.[12,13,16] Despite the unique breadth of these broadly neutralizing anti-HA antibodies, several viral mutations have been reported to impair the antibody binding and function. For example, the HA mutation A388V was shown to impair the binding of bNAbs that bind the HA stem, and head mutations that can make the virus completely resistant to strain-specific antibodies can also enable the virus to escape bNAbs that target the same region.[17,18] The other major surface glycoprotein of influenza virus, the neuraminidase (NA), has been recently suggested as a promising target for bNAbs.[19] NA is an enzyme that cleaves the sialoside receptor from the cell surface and enables the progeny virus to be released from the infected cell during viral budding.[20] As the NA exhibits a slower antigenic drift

Received 9 April 2024; accepted 28 July 2024;
https://doi.org/10.1016/j.ymthe.2024.07.023.

Correspondence: Yotam Bar-On, Department of Immunology, Rappaport Faculty of Medicine, Technion-Israel Institute of Technology, Haifa 3525422, Israel.
E-mail: ybaron@technion.ac.il

Please cite this article in press as: Moirangthem et al., Dual neutralization of influenza virus hemagglutinin and neuraminidase by a bispecific antibody leads to improved antiviral activity, Molecular Therapy (2024), https://doi.org/10.1016/j.ymthe.2024.07.023

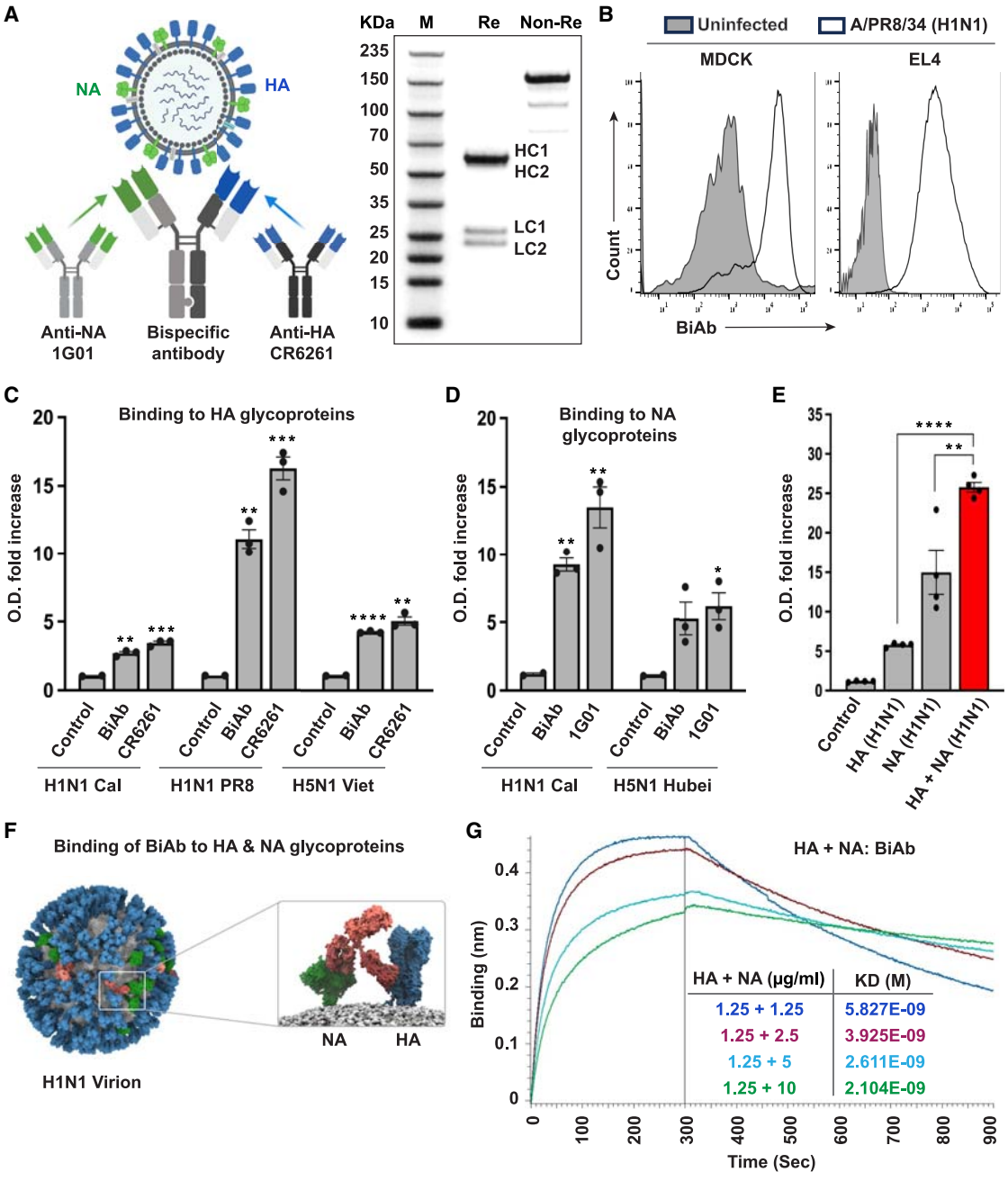

Figure 1. Binding of the BiAb to the HA and NA glycoproteins

(A) Schematic representation of the BiAb and SDS-PAGE analysis of the purified BiAb under reducing and non-reducing conditions. Re, reducing conditions; Non-Re, non-reducing; HC, heavy chain; LC, light chain. (B) FACS staining of infected cells and influenza virus-coated cells. The right histogram shows the binding of the BiAb to virion-coated EL4 cells, and the left histogram shows the BiAb binding to influenza virus-infected cells (H1N1 A/PR/8/34). Gray histograms depict the binding of the BiAb to uninfected or uncoated cells. The figure shows a representative staining. Four independent experiments were performed. (C–E) Analysis of the BiAb binding in ELISA. ELISA plates were coated with 0.5 µg of HA glycoproteins, 0.5 µg of NA glycoprotein, or 0.5 µg of a combination of HA + NA (0.25 µg each) and stained with the BiAb, CR6261, or 1G01. HA and NA were derived from different influenza virus strains (indicated in the x axis). The y axis depicts the fold changes in OD levels in comparison with the background OD values that were measured for each antibody or for the control wells. The black asterisks represent the statistically significant differences between the control and the antibodies (BiAb, CR6261, and 1G01) in (C) and (D) (*$p < 0.05$,**$p < 0.01$, ***$p < 0.001$, ****$p < 0.0001$, unpaired Student's t test) and between BiAb binding to both HA and NA or to a single glycoprotein in (E) (**$p < 0.01$, ****$p < 0.0001$, one-way ANOVA with Tukey's multiple comparison test). Data are represented as mean ± SEM ($n = 3$). The figure shows a representative staining out of three independent experiments that were performed. (F) A molecular dynamic stimulation. A model of full H1N1 virion bound

(legend continued on next page)

than the HA, bNAbs against this glycoprotein usually show broader cross-reactivity.[19]

Of note, the effect of dual-antibody targeting, in which both the HA and the NA are neutralized, has not been thoroughly tested. This is of special interest since it has been shown that a functional balance between HA and NA is required for efficient viral replication.[21–23] For example, reverse genetics studies showed that reduced fitness of influenza virus that resulted from an increased HA affinity could be restored by an increased NA activity.[21–23] Moreover, it was shown that mutations in the HA protein can lead to secondary mutations in the NA protein, and it has been suggested that the balance between the HA and NA activity has a great impact on viral growth and viral fitness.[21–23] Finally, it was recently shown that neutralization by anti-HA stem antibodies can also block the NA activity.[24] This was attributed to steric inhibition of the viral NA by the Fc region of anti-HA stem antibodies and provided another example for the close proximity of the viral NA and HA.[24]

The unique interplay of the HA and NA glycoproteins and our previous findings, in which we demonstrated the use of dual-antibody therapy for sustained viral suppression of highly mutable viruses,[9] prompted us to perform in-depth analysis of dual-antibody-mediated neutralization of the influenza virus HA and NA, especially as a combination of bNAbs was recently shown to be effective in both protecting and treating various viral infections, including influenza virus,[25] hepatitis B virus,[26] HIV-1,[3–6] and severe acute respiratory syndrome coronavirus 2 (SARS-CoV-2)[10] in both preclinical studies and in the clinic. The fact that antibody combination therapy was safe and tolerable, and in some cases was able to limit the emergence of the antibody-resistant viruses, has generated interest in applying this approach for controlling influenza infection, for which current therapeutics have shown limited success.[13] Here we generate a bispecific antibody (BiAb) that inhibits the HA and NA of various influenza virus strains and characterize its improved biological activity compared to a monoclonal antibodies (mAbs) combination.

RESULTS

Generation of a BiAb against the HA and NA and its binding to various influenza virus strains

To analyze the virological and immunological outcomes of the dual neutralization of HA and NA, we designed and generated a BiAb that inhibits both glycoproteins. The BiAb consists of the Fab regions of the stem-specific anti-HA bNAb CR6261[27] and the recently isolated anti-NA bNAb 1G01.[19] These antibodies were selected based on their exceptional breadth and potency.[19,28] The Fab regions were cloned into plasmids encoding the light chains and heavy chains with engineered Fc domains that promote heterodimerization.[29] The N399K and E356K mutations were introduced into the Fc domain of the CR6261 heavy chain, and the K409D and K392D were introduced into the Fc domain of the 1G01 heavy chain.[29]

Plasmids were used to transfect ExpiCHO cells; the BiAb was purified from the cell supernatant using protein A column, and antibody purity was evaluated by size exclusion-high-performance liquid chromatography (Figure S1A). The purified BiAb was also analyzed by SDS-PAGE (Figure 1A). ExpiCHO cells were also used to generate the monoclonal CR6261 and 1G01 antibodies (Figure S1B). Following BiAb purification, we infected Madin-Darby canine kidney (MDCK) cells with influenza virus A/Puerto Rico/8/1934 (H1N1) (PR8) and stained uninfected cells and influenza virus-infected cells 48 h following the infection. A significant increase in the BiAb staining was seen in the infected MDCK cells in comparison with uninfected cells (Figure 1B left). Next, we tested whether the BiAb can bind to influenza virus virions by coating EL4 cells with influenza virus A/Puerto Rico/8/1934 (H1N1). These cells cannot be infected by PR8 but allow viral attachment.[30] Influenza virus-coated cells were detected by the BiAb (Figure 1B right). Using ELISA, we demonstrated that the BiAb also binds isolated HA and NA from A/Puerto Rico/8/1934 (H1N1), A/California/04/2009 (H1N1), A/Vietnam/1194/2004 (H5N1), and A/Hubei/1/2010 (H5N1) (Figures 1C and 1D). Moreover, when the BiAb was incubated with both HA and NA, the levels of binding significantly increased (Figure 1E).

To test all possible antibody interaction sites with the H1N1 virion, we superimposed the HA-Fab complex and the NA-Fab on all the HA and NA molecules on the virion model from a molecular dynamic stimulation.[31,32] Next, pairs of Fabs (one bound to HA and the other to NA) that could be connected via the Fc domain into a complete immunoglobulin (Ig) G structure were identified (Figure 1F). This analysis suggests that a single BiAb can potentially engage both the HA and the NA. Moreover, we applied a biolayer interferometry (BLI) technology to first measure the affinity of the BiAb to both the HA (KD = 4.397E−09) and the NA (KD = 2.442E−08) and the affinity of the mAbs to the same antigens (Figures S1C–S1F). We further verified that the BiAb affinity increased under constant concentrations of the HA and increasing concentrations of the NA (Figure 1G), indicating that the NA-Fab of the BiAb can be engaged while the HA-Fab is bound by the HA antigen.

by the BiAb (left). viral membrane (gray), HA (blue), NA (green), and computationally predicted bound BiAb (coral). A zoomed image of a single BiAb bound to HA trimer and NA tetramer is shown on the right. (G) Measurement of the BiAb affinity. BLI was used to measure the binding affinity (K_D) of BiAb to HA and NA proteins. The biosensors were loaded together with a constant concentration of HA and an increasing NA protein concentration and incubated with the BiAb (100 nM) for 300 s at the association step followed by incubation in buffer for 120 s at the disassociation step as shown on the x axis. The changes of thickness at the tip of biosensors (response, nM) caused by antibody-antigen binding are shown by the y axis. The association-dissociation pattern and the binding constants are calculated from the resulting fitting curves based on a 1:1 binding model. Octet Analysis Studio was used to analyze the data. Graphs are color coded based on the NA concentration that was used. Calculated K_D (M) for each protein concentration is depicted in the figure.

Please cite this article in press as: Moirangthem et al., Dual neutralization of influenza virus hemagglutinin and neuraminidase by a bispecific antibody leads to improved antiviral activity, Molecular Therapy (2024), https://doi.org/10.1016/j.ymthe.2024.07.023

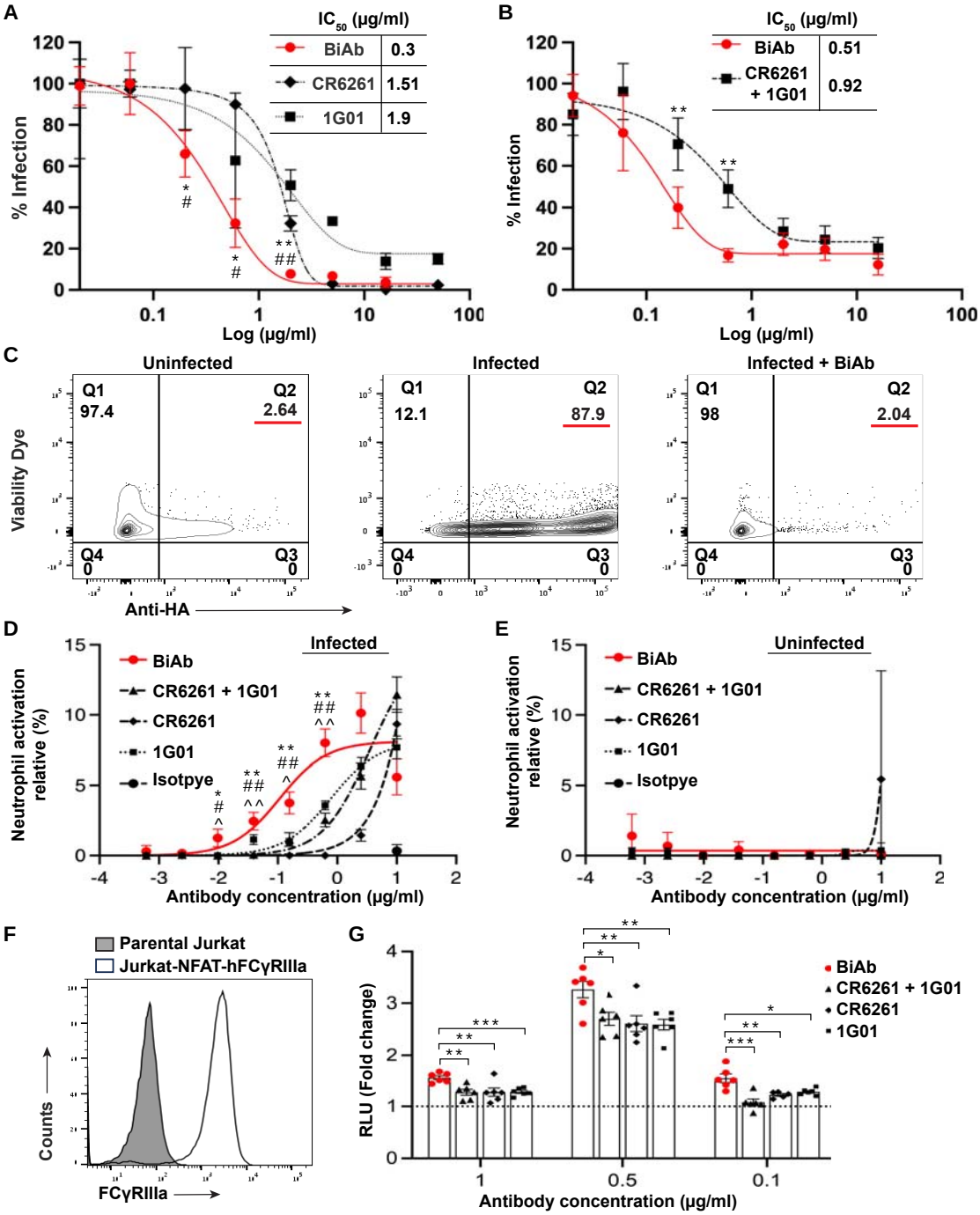

Figure 2. The dual-antiviral activity of the BiAb

(A and B) Neutralizing activity of the antibodies CR6261, 1G01, BiAb, or a combination of CR6261 and 1G01 against A/Puerto Rico/8/34 (H1N1) was assessed by a microneutralization assay. The virus was incubated with the antibodies CR6261, 1G01, BiAb, or a combination of CR6261 and 1G01. MDCK infection was evaluated by analyzing the expression of the influenza virus NP in the infected cells. To calculate the % infection, the results were compared to cells that were infected with influenza virus in the absence of antibodies. Antibody concentrations are indicated in the x axis. A summary of three independent experiments is shown and data were fitted using non-linear regression analysis (four parameter). Statistically significant differences between BiAb and CR6261(*$p < 0.05$, **<0.005, one-way ANOVA), BiAb and 1G01, (#$p < 0.05$, ##$p < 0.005$, one-way ANOVA), and BiAb and antibody combination (**$p < 0.005$, unpaired Student's t test) are shown. The IC_{50} values that are indicated in the figure were calculated based on the pooled data from all three experiments. Values were calculated using AAT Bioquest IC_{50} calculator (https://www.aatbio.com/tools/ic50-calculator).

(legend continued on next page)

Improved antiviral activity of the BiAb

We designed the BiAb with a "block and lock" antiviral activity based on the notion that blockade of the HA by the BiAb will prevent both viral entry into target cells and egress from infected cells. To test the BiAb neutralization, we incubated PR8 with serial dilutions of the BiAb, CR6261, or 1G01 and preformed a microneutralization assay using MDCK cells.[33] The BiAb demonstrated 5-fold lower half maximal inhibitory concentration (IC_{50}) (IC_{50} = 0.3 μg/mL) compared to either CR6261 (IC_{50} = 1.51 μg/mL) or 1G01 (IC_{50} = 1.9 μg/mL) (Figure 2A). Strikingly, BiAb neutralization was superior to a combination of CR6261 and 1G01 (IC_{50} = 0.92 μg/mL; Figure 2B). To determine whether BiAb inhibited virus release, we first confirmed the ability of the BiAb to neutralize the PR8 NA glycoprotein. A significant reduction was seen in the enzymatic activity of NA upon incubation with either the BiAb or 1G01 (Figure S2A). Furthermore, inhibition of the NA with 10 μg/mL oseltamivir (Tamiflu), a clinically used inhibitor of the NA, has led to a greater reduction in NA activity, which was not augmented by a combination with BiAb, 1G01, or CR6261 (Figure S2A). This is in accordance with previous publications that demonstrated that both 1G01 and oseltamivir target the same region (the active site) of the NA.[34,35] We next treated infected cells with the BiAb, 1G01, or CR6261 24 h after infection was established. Cells were washed, unbound antibodies were removed, and viruses from the cell supernatant were collected from the antibody-treated cells and untreated cells 48 h following infection. The collected viruses were then used to infect fresh MDCK cells, and the level of infection was evaluated after 48 h. Viruses that were collected from infected untreated MDCK cells resulted in a robust infection of the freshly thawed MDCK cells, while minimal or no infection was seen when viruses were collected from BiAb-treated infected cells (Figure 2C) or from 1G01-treated infected cells but not from CR6261-treated cells (Figure S2B). We concluded that the BiAb shows high neutralization capacity and is also capable of preventing the budding of newly formed viruses from infected cells. We postulated that improved neutralization of the BiAb compared to a combination of the CR6261 and 1G01 antibodies (Figure 2B) could be due to steric inhibition caused by anti-stem HA antibodies that block access to the influenza NA glycoprotein as shown by Kosik et al.[24] and others.[36] To validate this hypothesis, PR8-infected MDCK cells were preincubated with CR6261 or left untreated and were then stained with the 1G01 antibody. Preincubation of the infected cells with CR6261 significantly reduced the binding of 1G01 to the surface of infected cells, and this was dependent on the concentration of 1G01 that was used for the staining (Figure S2C).

We next compared the ability of the BiAb, CR6261, and 1G01 to engage the human Fc receptor CD32a.[35] We co-cultured mouse neutrophils isolated from the bone marrow of mice lacking all endogenous FcγRs and transgenic for human CD32a with PR8-infected MDCK cells incubated with serial dilutions of the BiAb, CR6261, 1G01, or a combination of CR6261 and 1G01. Activated neutrophils were identified by flow cytometry as Ly6G-positive cells that had shed CD62L and upregulated CD11b.[37] Although no neutrophil activation was observed upon incubation with antibodies and uninfected MDCK cells, incubation with infected cells in the presence of any HA- or NA-targeting antibody triggered neutrophil activation at antibody concentration of 1 μg/mL (Figures 2D and 2E). Importantly, incubation with the BiAb led to a significantly higher percentage of activated neutrophils in comparison with CR6261, 1G01, or their combination across different antibody concentrations, with the differences being the most pronounced at low antibody concentrations (Figure 2D).

Additionally, since natural killer (NK) cells express the Fc receptor CD16 (FcγRIIIa) and because they play a major role in the antiviral response against influenza virus,[38] we further tested the ability of the BiAb to engage the human Fc receptor FcγRIIIa. Uninfected and influenza virus-infected cells were incubated with CR6261, 1G01, their combination, or the BiAb and cultured with Jurkat NFAT CD16 reporter cells stably expressing the human FcγRIIIa (Figure 2F). Despite the relatively low affinity of mouse IgG1 to human FcγRIIIa,[39] all the tested antibodies were able to activate the human FcγRIIIa to some extent (Figure 2G). Importantly, the BiAb was able to elicit a significantly stronger activation of human FcγRIIIa in comparison with CR6261, 1G01, or their combination across different concentrations of the antibodies (Figure 2G). These data show that the BiAb has a stronger potential to trigger Fc-dependent cell activation at low antibody concentrations and demonstrate that it can better engage human CD32a or human FcγRIIIa to induce neutrophil or NK cell activation in comparison with a combination of the mAbs.

Dual neutralization of the HA and NA alters the mutation landscape of influenza virus

Antigenic drift in both HA and NA plays a dominant role in the short duration of immunity to influenza virus.[40] To examine how a

(C) Plots that depict the percentage of infected cells (HA-positive cells) in MDCK cells that were incubated with supernatant from infected cells (middle panel) or incubated with supernatant from infected cells that were treated with the BiAb (right panel). The number in each Q2 quadrant depicts the percentage of influenza virus-infected cells. One representative experiment is shown out of three performed. (D and E) Percentage of neutrophil activation following incubation of H1N1-infected (D) and uninfected (E) MDCK cells with BiAb, CR6261, 1G01, or a combination of CR6261 + 1G01. The antibody concentration is depicted in the x axis. Relative neutrophile activation (%) was measured by analyzing CD62L shedding and CD11b upregulation after subtraction of the values that were observed with no target cells but with the addition of the antibodies. Statistically significant difference between BiAb and CR6261 (*$p < 0.05$, **<0.005), BiAb and 1G01 (#$p < 0.05$. ##$p < 0.005$), and BiAb and combination (^$p < 0.05$, ^^$p < 0.005$) are shown; one-way ANOVA with Tukey's multiple comparison test. Shown is one representative experiment out of three preformed. (F) Staining of parental Jurkat cells (dark gray histogram) and Jurkat NFAT FcγRIIIa cells (empty histogram) with anti-human CD16 Ab. Shown are representative histograms out of three independent experiments that were preformed. (G) Luminescence values following incubation of Jurkat NFAT CD16 cells with PR8-infected MDCK cells. Shown are fold changes of the luminescence values and the luminescence values seen for each antibody when used in uninfected MDCK cells was used as control and set as 1 (dashed line). Shown is one representative experiment out of three performed. Each dot depicts a tested well. Data represent mean ± SEM. Statistically significant differences are shown (*$p < 0.05$, **$p < 0.005$, ***$p < 0.001$, one-way ANOVA with Tukey's multiple comparison test).

Please cite this article in press as: Moirangthem et al., Dual neutralization of influenza virus hemagglutinin and neuraminidase by a bispecific antibody leads to improved antiviral activity, Molecular Therapy (2024), https://doi.org/10.1016/j.ymthe.2024.07.023

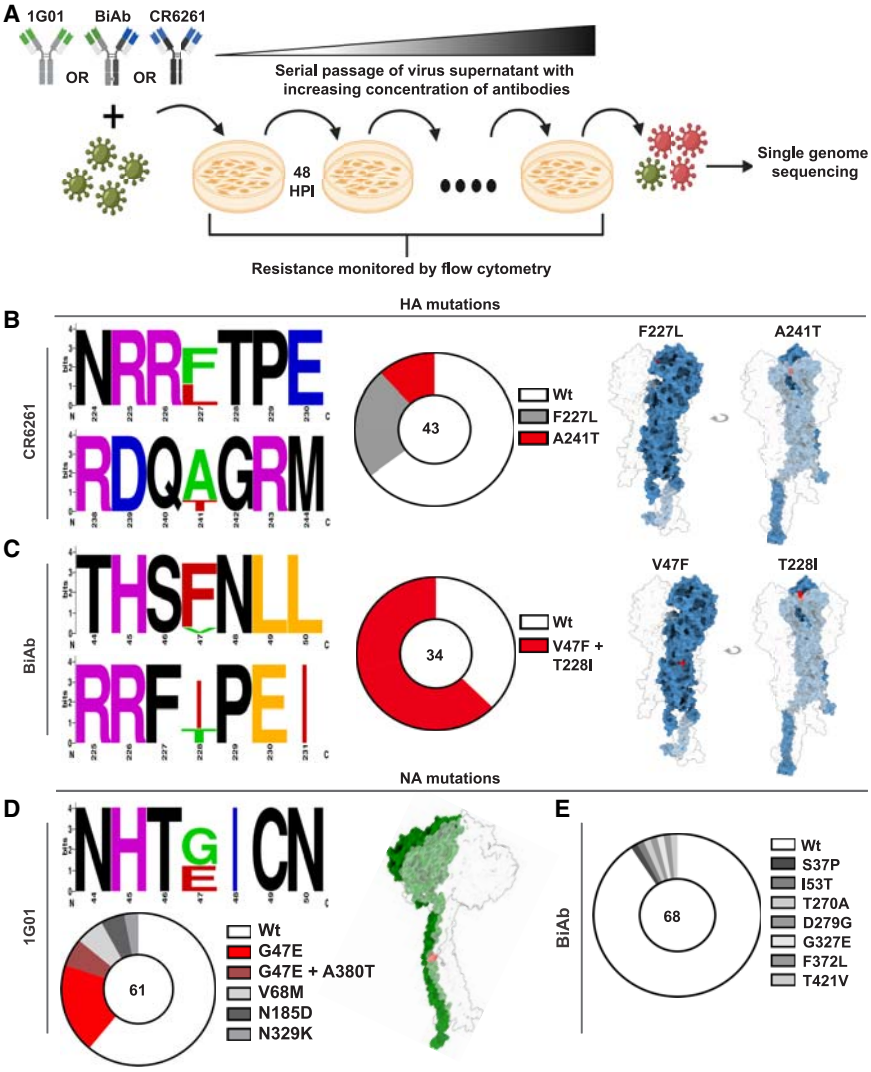

Figure 3. Mutation profile of the HA and NA proteins

(A) Schematic presentation of serial passage of A/Puerto Rico/8/34 (H1N1) with CR6261 or BiAb; HPI-hours post infection. (B–E) Logo plots and pie charts of SGS derived from viruses following serial passage with CR6261 (B), 1G01 (D), or BiAb (C and E). The frequency of viruses carrying a specific mutation in the HA or NA is shown by the height of the letter colored in red. The numbers in the x axis depict the amino acid location in the A/Puerto Rico/8/34 HA and NA glycoproteins. The figures were made using the web logo (https://weblogo.berkeley.edu/logo.cgi). The y axis height specifies the number of bits, which indicates the information content of a sequence position. By default, the height of the y axis is the maximum entropy for the given sequence type (log2 20 = 4.3 bits for protein). The pie charts show the percentage of viruses that carry the indicated mutations in the HA (B and C) or NA (D and E). The number in the middle of the pie chart depicts the total number of viruses that were analyzed by SGS in each analysis. The white pie slice represents unmutated HA or NA sequences. The colored pie slices represent the acquired mutations of HA or NA as indicated in the figure. Locations of amino acid substitutions (red) on the HA trimer and the NA tetramer structure were identified using UCSF ChimeraX. The SGS was done once for the HA analysis and once for the NA analysis.

bifunctional antibody alters the HA escape repertoire, we passaged PR8 10 times in the presence of increasing amounts of CR6261 or BiAb and performed single-genome sequencing (SGS) of the HA gene (Figure 3A).[41] We isolated 43 viruses following exposure to CR6261, from which 16 carried an F227L mutation in the HA and eight carried A241T mutation in the HA (Figure 3B). Altogether, 24 viruses carried a single mutation in the viral HA and no virus was shown to express the two mutations simultaneously (Figure 3B). In contrast, exposure of the virus to the BiAb has resulted in variants that carry a dual-HA mutation V47F and T228I (Figure 3C). Additionally, by analyzing the antibody neutralization activity, we demonstrated that both the mutations that emerged following exposure to CR6261 or the BiAb led to reduced sensitivity of the virus to antibody neutralization (Figures S3A–S3C). Thus, we conclude that, although the influenza virus can develop resistance mutation against the BiAb, the selective pressure that is mediated by dual neutralization of the HA and the NA alters the HA mutation landscape of the virus compared to mutations seen following single neutralization of the HA.

The sharp difference in the HA mutation profile following exposure of PR8 to CR6261 or to the BiAb has led us to further investigate the nature of the HA mutations that were captured by our SGS analysis. The HA RBS is formed by three structural elements at the tip of the HA molecule, an α helix composed by residues 190–198 (the 190 helix) and two loop structures formed by residues 133–138 (the 130 loop) and 220–229 (the 220 loop).[42,43] Interestingly, while exposure to both the CR6261 and the BiAb has led to mutations in the HA RBS (F227L and T228I), exposure to the BiAb has resulted in variants that carry an additional mutation in the HA stalk region (V47F), which is a relatively conserved region of the HA (Figures 3B and 3C). Interestingly, none of these mutations was identified in circulating influenza virus H1 strains that are documented in GISAID (during 2013–2023), suggesting that such mutations might impair the viral fitness and transmissibility. Furthermore, the fact that all BiAb-escape mutants carried a dual mutation in the HA glycoprotein is consistent with the idea that HA escape from the BiAb requires additional structural changes compared to individual anti-stem Abs. To investigate the effects of these escape mutations on the influenza virus, we cloned the mutated HA proteins that we identified and fused these mutated HAs with the human IgG1 Fc domain. These constructs were used to transfect ExpiCHO cells,

and purified fusion proteins were evaluated by SDS-PAGE (Figure S4A). We then compared the binding of wild-type (WT) HA-Ig and the mutated HA-Ig proteins (F227L-Ig, A241T-Ig, and V47F + T228I-Ig) to MDCK cells. A significant reduction in HA binding to MDCK cells was seen in all three mutants in comparison with the binding of WT HA-Ig, indicating that viral escape from the CR6261 and the BiAb antibodies resulted in altered binding capacity of the mutated HAs to sialic acid residues that are expressed on the membrane of the MDCK target cells (Figures S4B and S4C).

Next, we performed SGS analysis to identify possible changes in NA mutations following exposure to 1G01 or to the BiAb by using the rolling culture described above. Following incubation with 1G01, a large portion of the isolated viruses (25 viruses out of 61 viruses that were analyzed) developed a G47E substitution in the NA hypervariable stalk region (Figure 3D). Strikingly, despite analyzing a large number of NA genes from single virions ($n = 68$), no specific accumulation of NA mutants was recorded following exposure to the BiAb and only sparse mutations were seen (Figure 3E). This further indicates that the dual neutralization of the HA and the NA can alter and limit the mutation landscape of the HA and NA glycoproteins compared to single neutralization of one of these glycoproteins.

BiAb exhibit improved protective and therapeutic activity in influenza virus-infected mice

Based on the enhanced viral neutralization activity of BiAb, its enhanced neutralization capacity, and its augmented Fc-mediated functions (Figure 2), we next evaluated the protective capacity of BiAb in lethally PR8-infected C57BL/6 mice. Administration of CR6261 at 15 mg/kg was previously shown to prevent weight loss and significantly improve survival of influenza virus-infected mice.[44] In preliminary experiments, 6 mg/kg of CR6261 given intraperitoneally (i.p.) to mice 4 h after infection effectively prevented weight loss with 85% survival (Figures S5A and S5B), while 2 mg/kg CR6261 failed to prevent weight loss with 30% survival (Figures S5A and S5B). Thus, we chose the 2 mg/kg mAb dose to compare the antiviral activities of CR6261, 1G01, and BiAb. Initially, we verified the safety of administrating the BiAb at 2 mg/kg i.p. by following any side effects during a span of 2 weeks following antibody administration. No side effects were recorded, and the BiAb-treated mice gradually gained weight (Figure 4A). We also evaluated the BiAb pharmacokinetics in mice and demonstrated that the BiAb has a half-life ($t_{1/2}$) of 6.1 days (Figure 4B). Furthermore, the neutralization activity of the BiAb was also evaluated *in vivo* by administrating the BiAb (2 mg/kg), by infected the mice 4 h after antibody administration, and by testing the levels of influenza virus-infected lung epithelial cells at early time points after the infection. A significant increase in influenza virus-infected lung epithelial cells was observed in the infected mice at day 3 and day 4 of infection (Figures S6A–S6D). However, this increase was significantly lower in the lungs of mice that were administered the BiAb compared to the untreated infected mice (Figures S6B–S6D).

Consistent with our *in vitro* findings (Figures 1 and 2), the BiAb demonstrated increased protection compared to CR626, 1G01, or a combination of CR6261 and 1G01 ($n = 21$ per group) with a decreased weight loss and significantly reduced pulmonary viral loads (Figures 4C–4E and S7). Moreover, mice that were administered the BiAb 4 h prior to infection showed improved survival compared to mice administered CR6261 or 1G01. A significantly improved survival was also recorded in these mice in comparison with the combination of CR6261 and 1G01, albeit to a lesser extent (Figure 4F).

Since antibodies are usually administered following infection and not as a preventive measure,[10,12,45] we next evaluated the antibodies in a therapy model. Mice were infected with three different strains of influenza virus that were previously shown to effectively infect mice: A/Puerto Rico/8/1934 (H1N1), A/FortMonmouth/1/1947 (H1N1), and A/Wilson-Smith/1933 (H1N1). The ability of the BiAb to recognize and neutralize the different influenza strain was first verified *in vitro* (Figures S8A and S8B). Mice were then administered CR6261, 1G01, BiAb, or a combination of CR6261 and 1G01 ($n = 20$ per group) 2 days following the infection. Following infection with all of the tested strains, antibody therapy with the BiAb led to a more moderate weight loss in comparison with mice treated with a combination of CR6261 and 1G01 (Figure 5) and this was evident mostly in the mice that were infected with A/Puerto Rico/8/1934 (H1N1). Importantly, in mice infected with A/Puerto Rico/8/1934 (H1N1) or A/Wilson-Smith/1933 (H1N1), only the BiAb treatment led to significant increase in mice survival (Figures 5B and 5F). All other antibody-treated groups as well as the antibody combination-treated group failed to significantly improve the mouse survival compared to the untreated mice (Figures 5B and 5F). Moreover, in A/FortMonmouth/1/1947 (H1N1)-infected mice, increase in mouse survival was seen in mice treated with the BiAb, 1G01, and a combination of CR6261 and 1G01 compared to untreated mice (Figure 5D). Nevertheless, BiAb treatment led to the most pronounced increase in the survival rate (BiAb = 75%, 1G01 = 47.05%, CR6261 and 1G01combination = 42.1%), which was also significantly higher than the survival rate of mice treated with a combination of CR6261 and 1G01 (Figure 5D, $p = 0.02$). We concluded that dual neutralization of the HA and NA by the BiAb can improve antibody-based control of various influenza viruses.

To further investigate the increased efficacy that was observed with BiAb therapy, we also analyzed cellular immune response in the lungs of mice that were infected with A/Puerto Rico/8/1934 (H1N1) and were treated with 2 mg/kg of BiAb 2 days after the infection. Mouse lungs were harvested at various time points after the infection to profile the lung $CD3^+CD4^+$ cells and the lung $CD3^+CD8^+$ cells by flow cytometry (Figure S9). Analysis of the lung T cells revealed that administration of the BiAb during infection has no significant effects on the percentage of the lung $CD3^+CD4^+$ cells and the lung $CD3^+CD8^+$ in all of the tested time points (Figure S9A). However, the levels of activated $CD69^+CD4^+$ T cells in the lungs were significantly increased in the BiAb-treated mice at day 5 and day 7.

Please cite this article in press as: Moirangthem et al., Dual neutralization of influenza virus hemagglutinin and neuraminidase by a bispecific antibody leads to improved antiviral activity, Molecular Therapy (2024), https://doi.org/10.1016/j.ymthe.2024.07.023

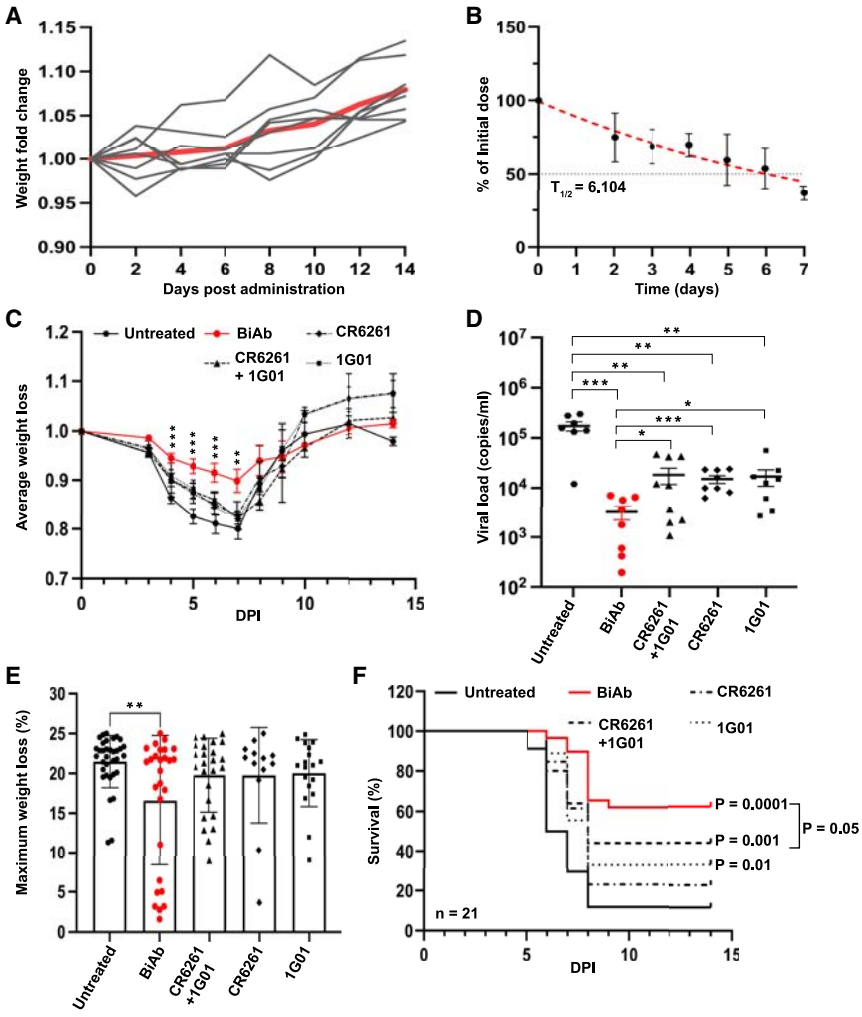

Figure 4. Assessment of the prophylactic efficacy of the BiAb in comparison with CR6261, 1G01, and antibody combination

(A) Mouse weight following BiAb administration. Mouse weights were evaluated following administration of the BiAb at 2 mg/kg i.p. (n = 8). The mouse weights at day 0 were set as 1. Gray graphs depict the weight fold change of individual mice, and the red graph depicts the average mouse weight fold change. (B) BiAb plasma half-life measurements. The y axis depicts the percentage of the BiAb in mouse plasma out of the initial antibody dose. Dots and error bars depict the average measurements in three mice. The red dashed graph depicts the calculated non-linear regression. The black dashed line depicts 50% of the initial antibody dose. The calculated antibody half-life is shown in the figure ($t_{1/2}$). (C–E) Mouse weight loss and lung viral titers following infection. Mouse weight loss (C) and viral titers (at day 7) in the lungs (D) were evaluated following infection with the 4.6 × 10^3 PFU/mL of A/Puerto Rico/8/34 (H1N1) influenza virus 4 h after the administration of 2 mg/kg of the BiAb, CR6261, 1G01, or a combination of CR6261 and 1G01. Weight loss of the BiAb-treated mice was compared to untreated mice using unpaired Student's t test (**p < 0.005, ***p < 0.001) and viral loads were compared by one-way ANOVA (Tukey's multiple comparison test; *p < 0.05, **p < 0.005, ***p < 0.001). In (D), each data point depicts an individual mouse, and mice with no detectable viral load or mice that were found dead at day 7 were excluded from the analysis. (E and F) Maximal mouse weight loss (E) and % survival (F) following infection with the 4.6 × 10^3 PFU/mL of A/Puerto Rico/8/34 (H1N1) influenza virus and administration of 2 mg/kg of the BiAb, CR6261, 1G01, a combination of CR6261 and 1G01, or in untreated mice. Antibodies were administered 4 h before infection by i.p. injection. The data are a summary of three independent experiments, and at least 21 mice were infected in each group. In (E), maximal weight loss was calculated by dividing the minimal weight of each mouse with the weight of each mouse at day 0. Each data point depicts an individual mouse. Data shown are means ± SEM (**p < 0.005, unpaired Student's t test). (F) Kaplan-Meier survival plots. In the survival curve, the average number of mice in each group is n = 21, and mice losing 25% of their initial weight were sacrificed. Statistically significant differences between antibody-treated groups and the untreated group are indicated in the figure (p values) and were calculated by the log rank test. The statistical differences between BiAb-treated mice and a combination of CR6261 and 1G01 were determined by Gehan-Breslow-Wilcoxon test.

Similarly, the BiAb-treated mice showed augmented levels of activated $CD69^+CD8^+$ T cells in the lungs at day 5 (Figures S9B–S9E). This implies a possible effect of BiAb administration on the activation state of lung T cells during the course of influenza virus infection.

DISCUSSION

Unlike other enveloped RNA viruses that are circulating in the human population, such as HIV-1 and SARS-CoV-2, that contain only one dominant surface protein, the influenza virus has two highly immunogenic surface proteins that can be targeted by antibodies.[46,47] In this work, we uncovered several advantages of dual-antibody neutralization of the influenza virus HA and NA. First, as the HA viral glycoprotein is responsible for viral entry to the target cells and the NA facilitates the budding of the newly formed viruses from the infected cells,[48] we show that the BiAb can inhibit the viral entry to the target cells and the release of new virions from the infected cells. Second, we demonstrated that dual neutralization of the HA and NA results in improved viral neutralization compared to neutralization of only the HA glycoprotein, which is considered the dominant viral protein that facilitates viral infection. We postulate that the enhanced neutralization activity of the BiAb is due to the multifunctional role of the NA in the influenza virus life cycle.[49] As the role of the NA in releasing progeny viruses from the infected epithelial cells is well documented and described, additional studies have suggested that NA may play other roles in the viral attachment and entry to the target cells.[20,24,46,49,50] In agreement with this, we and others demonstrated that neutralizing antibodies against the NA can also impair viral infection. Finally, we reveal that the influenza virus has the

Please cite this article in press as: Moirangthem et al., Dual neutralization of influenza virus hemagglutinin and neuraminidase by a bispecific antibody leads to improved antiviral activity, Molecular Therapy (2024), https://doi.org/10.1016/j.ymthe.2024.07.023

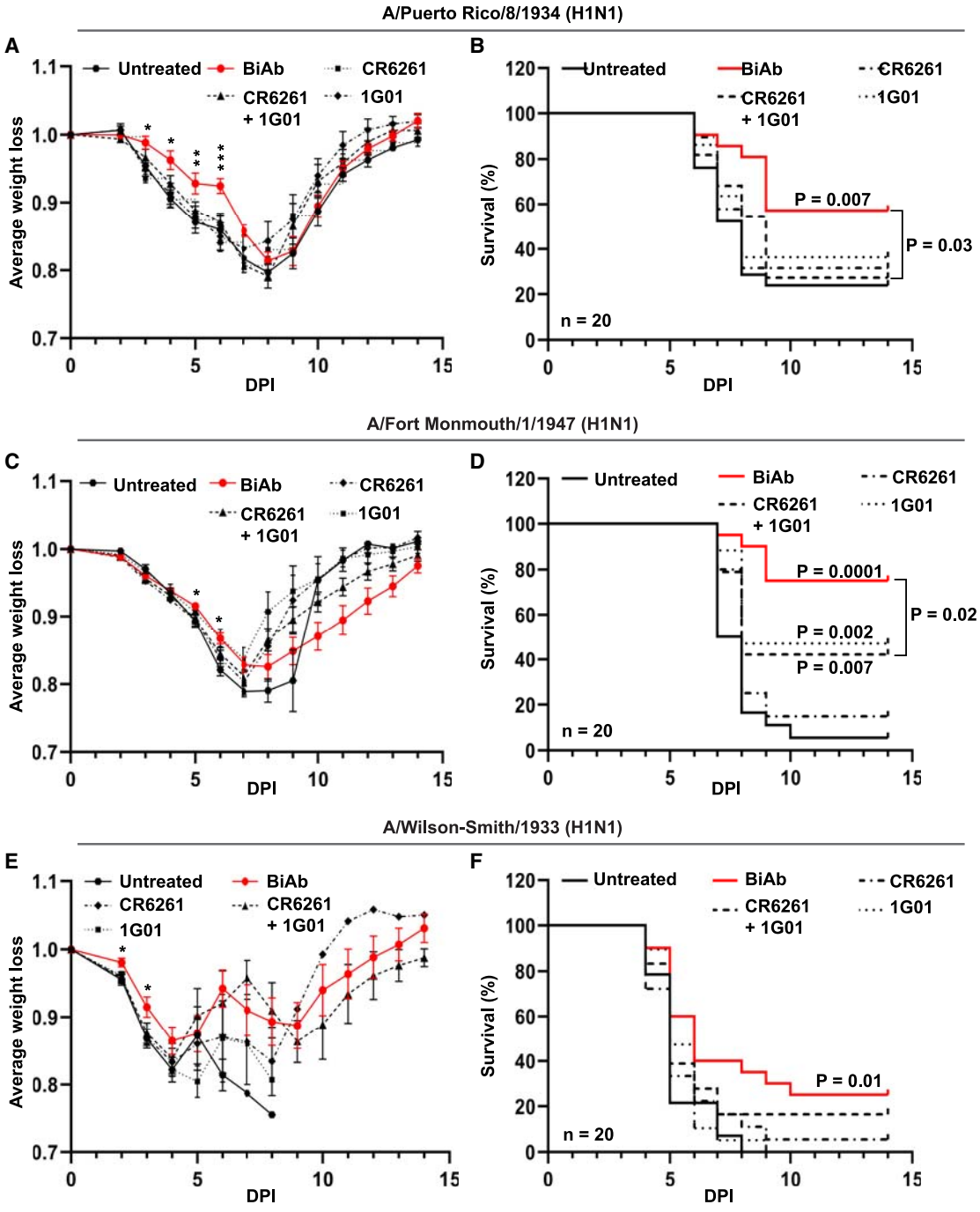

Figure 5. Testing the therapeutic efficacy of the BiAb in comparison with CR6261, 1G01, and antibody combination

(A, C, and E) Mouse weight loss following infection with 4.6×10^3 PFU/mL of various influenza virus strains and following administration of antibodies (2 mg/kg) 2 days following the infection. The virus strain and the antibodies that were used are indicated in the figure. Weight loss was calculated by dividing the weight of each mouse by the weight of the individual mouse at day 0. Shown are the mean weight loss values ±SEM. The x axis depicts the days post infection (DPI). BiAb-treated mouse weight loss was compared to the combination-treated mice using unpaired Student's t test (*$p < 0.05$, **$p < 0.005$, ***$p < 0.0005$). (B, D, and F) Kaplan-Meier survival plots depicting mouse survival (%) following infection with 4.6×10^3 PFU/mL of the influenza virus strain and following administration of antibodies (2 mg/kg) 2 days following the infection. The virus

(legend continued on next page)

ability to escape the BiAb, even though the mutation landscape that resulted from exposure to the BiAb differs from single neutralization of the HA or the NA. This was most evident when analyzing the NA mutations, in which accumulation of G47E NA mutants was seen following exposure to 1G01 and was not seen after incubation with the BiAb. Notably, this mutation is far removed from the antibody-binding site and is located in the NA stalk region, which was previously shown to affect the NA tetramer stability.[47,51] Thus, we speculate that such a mutation may alter the tetrameric conformations of the NA and affect 1G01 accessibility to its NA binding site.

Additional work is required to uncover the mechanism by which the HA mutations that we identified result in antibody resistance in order to design an antibody combination that will better limit the emergence of resistant viral strains. In this regard, the sequencing of the viruses from the BiAb-treated mice could provide additional information about the varied responses that were seen in the weight loss of the infected mice following treatment. Moreover, such *de novo* mutation analysis could provide a more precise prediction of key resistance mutations, given that mutations that were observed in our *in vitro* system can be skewed by cell-line-specific viral mutations and by the lack of immune selection pressure. It will also be important to investigate whether HA mutants with reduced ability to bind their target cells that were identified in our *in vitro* assay are also developed *in vivo*. Given the unique interplay of the HA and NA,[23] it is also essential to identify combinations of HA and NA antibodies with synergetic activity in which escape mutations that arise in one glycoprotein can render the other protein more susceptible to antibody neutralization or impair its activity. In this regard, the BiAb also provides a unique research tool to study the importance of the competitive cooperation between HA and NA during viral entry and during the release of progeny viruses.

Finally, our observation in which we demonstrate that the BiAb-treated mice show increased lung T cell activation raises several important questions. Previous seminal studies have demonstrated that passive immunization with antibodies in chronic infections or conditions can result in a vaccinal effect in which the antibody enhances the cellular T cell activity.[4,52–54] Whether the vaccinal effect is responsible for the increased T cell activation that we observed during acute infection, as well as the importance of the targeted antigens and the lung viral loads in this process, remains to be tested.

One clear advantage of using a bispecific for neutralizing the HA and NA over a combination of two mAbs is that the generation of a BiAb is more economical.[55] Nevertheless, this work highlights functional differences in the activity of BiAb that target the HA and NA compared to antibody combination. In particular, we observed that the BiAb has an improved neutralization activity and an augmented ability to engage Fc receptors in comparison with a combination of the CR6261 and 1G01 antibodies. The reasons for these differences are not clear. Since the CR6261 antibody is directed against the stem of the HA, and because the Fc portion (50 kDa) of the anti-stem antibodies was shown to sterically inhibit the NA,[24,36] we hypothesize that a possible explanation for the improved activity of the BiAb over CR6261 and 1G01 is the steric inhibition of the NA by CR6261, which hinders the binding of 1G01 to the NA. Alternatively, these differences could also be attributed to a more synchronized neutralization of the HA and NA by the BiAb in comparison with a combination of CR6261 and 1G01; however, we did not address this possibility and it should be further evaluated in additional experiments. Namely, BLI data, ELISA experiments, and the structural modeling we performed suggest that the BiAb can engage both the HA and the NA simultaneously. However, additional experiments with cryogenic electron microscopy or crystallography are essential for a definite demonstration of such dual binding. Such structural mapping is of special importance given that the ELISA and BLI data provided indicate that engagement of the two BiAb Fab regions can occur simultaneously. Moreover, the structural modeling, in which we mapped all possible BiAb interaction sites with the H1N1 virion, further supports this claim. However, all of these experiments do not provide an experimental evidence for such BiAb binding on virions or on the surface of infected cells.

Antibody combination therapy has been extensively studied against HIV-1, hepatitis B virus (HBV), and SARS-CoV-2.[9,56,57] However, a thorough evolution of a dual-antibody neutralization of the HA and NA during influenza virus infection has not been performed despite the initial finding by Marathe et al. that a combination of anti-HA and anti-NA antibodies improves the survival of immunosuppressed mice following lethal infection with influenza B virus.[25] The recent isolation of neutralizing NA antibodies with their exceptional breadth to multiple different influenza A and B viruses from an H3N2-infected donor has paved the way for effective neutralization of the NA and for a combination therapy in which both the HA and the NA are neutralized.[19] Additional recent studies have highlighted the NA as an emerging target for influenza therapy and vaccines.[47] Out of the different NA antibodies that were isolated, the 1G01 antibody has the highest number of somatic hypermutations exhibiting the broadest binding,[19] which prompts us to combine this antibody with the CR6261 that binds the HA of most group-1 influenza viruses. Alternatively, dual inhibition of the HA and NA can also be achieved by antiviral drugs, as anti-NA inhibitors are commonly used in the clinic for treating influenza virus infection.[58–60] Our data in which we demonstrated no synergistic effect on NA inhibition by the BiAb and oseltamivir stress the need to identify

strain, the antibodies that were used, and the number of mice in each group (n = 20) are indicated in the figure. Statistically significant differences between the antibody-treated groups and the untreated group are indicated in the figure (p values) and were calculated by the log rank test. The statistical differences between BiAb-treated mice and a combination of CR6261 and 1G01 were also determined by a log rank test and are indicated in the figure (p values). The upper panel depicts infection with A/Puerto Rico/8/1934 (H1N1); the middle panel depicts infection with A/FortMonmouth/1/1947 (H1N1); the lower panel depicts infection with A/Wilson-Smith/1933 (H1N1).

the HA and NA epitopes that can be targeted by a BiAb for an optimal combination with current antiviral therapeutics.

MATERIALS AND METHODS

Study design

The aim of this study was to evaluate the effects of dual neutralization of influenza virus HA and NA glycoprotein on the course of influenza virus infection and on the host antiviral immune responses. A BiAb that neutralizes the HA and NA of various influenza virus strains was generated, and its antiviral activities were characterized by a variety of methods, including microneutralization assay, ELISA, flow cytometry, biolayer interferometry, and structural modeling. In addition, the therapeutic potential of the BiAb was thoroughly tested in influenza virus-infected mice by following the mouse weight loss, mouse survival, and virus titers in the lungs. The protective and therapeutic capacity of the BiAb at 2 mg/kg (i.p. injection) was compared to antibody monotherapy and to dual-antibody therapy using a similar dosage of 2 mg/kg. Mice that were not infected due to technical issues were not included in the analysis. Mice were randomly assigned to treatments, and investigators performing the immunological analyses were not blinded. Sample sizes were chosen on the basis of previous experiments in which influenza virus infection in mice was used. All animal experiments were approved by the Technion Animal Care and Use Committee.

Cell lines

The cell lines used in this study were the human alveolar basal epithelial cells (A549, ATCC # CRM-CCL-185), MDCK cells (ATCC # CCL-34), T lymphoblasts (EL4, ATCC # TIB-39), primary mouse neutrophils that were engineered to stably express the human CD32a,[61] Jurkat NFAT CD16 reporter cells (InvivoGen, catalog no. jktl-nfat-cd16), and ExpiCHO-S cells (Thermo Fisher, catalog no. A29133). Cells were maintained in culture at 37°C, 5% CO_2 in DMEM or RPMI 1640 medium supplemented with 4,500 mg/L D-glucose, 4 mM L-glutamine, 110 mg/L sodium pyruvate, 10% fetal bovine serum (FBS), 1% penicillin-streptomycin, and 1% nonessential amino acids (NEAAs). ExpiCHO-S cells were cultured in ExpiCHO-S cell expression medium (Thermo Fisher, A2910001) and maintained in an 8% CO_2 incubator at 37°C and 120 rpm.

Viral strains and recombinant proteins

Influenza viruses used in this study were A/Puerto Rico/8/1934 (PR8; H1N1), A/WS/33 H1N1 (ATCC, VR-219), and A/FM/1/47 H1N1 (ATCC, VR-97). The viruses were grown in eggs as previously described[30,62] and were further propagated in MDCK cells for 3–4 days at 37°C. The viral titer was then determined by plaque assay using MDCK cells.[63] Recombinant HA and NA glycoproteins used for ELISAs were purchased from Sino Biological. The HA proteins were from influenza A H1N1 (A/California/04/2009) (catalog no. 11055-V08B1), influenza A H1N1 (A/Puerto Rico/8/1934) (catalog no. 11684-V08H), influenza A H5N1 (A/Vietnam/1194/2004) (catalog no. 11062-V08H1), and NA proteins from influenza A H1N1 (A/California/04/2009) (catalog no. 11058-V08B) and influenza A H5N1 (A/Hubei/1/2010) (catalog no. 40018-V07H).

mAb and fusion protein generation

The NCBI IgBlast tool was used to determine the VDJ sequences of the heavy and light chains of CR6261 and 1G01. The variable heavy- and light-chain sequences of CR6261 and 1G01 were ordered as gBlocks (IDT) and subcloned into mammalian expression vectors[64] with mouse IgG1 heavy chain and mouse κ light chains, respectively. The sequences of the cloned plasmids were verified by restriction enzyme analysis and Sanger sequencing. Recombinant IgG antibodies were generated by transfecting the heavy-chain and light-chain constructs into an ExpiCHO cells Expression System (Thermo Fisher, catalog no. A29133) following the manufacture's Max Titer protocol. The supernatants were collected after 5–7 days of transfection and purified by affinity purification using protein G agarose beads (Pierce, catalog no. 89927). Purified proteins were dialyzed overnight in 1× PBS, filter sterilized (0.22 μm), and purity was assessed by SDS-PAGE followed by staining using InstantBlue Coomassie protein stain (Abcam, catalog no. ab119211). HA-Ig fusion proteins were generated by cloning the extracellular domain of PR8 HA or mutated HAs into a mammalian expression vector containing a mutation in the human IgG1 Fc domain.[65] Fusion proteins were then produced by using the ExpiCHO cells Expression System described above. The purity of the fusion proteins was assessed by SDS-PAGE before use.

BiAb design and production

Plasmids containing the heavy and light chain of the mAbs CR6261 and 1G01 were prepared as described above. The variable regions of CR6261 and 1G01 were codon optimized, synthesized, and cloned into an expression vector construct, pcDNA3.4, which has mouse IgG1 Fc. Four plasmids corresponding to the heavy and light chains of the mAbs were transiently co-transfected in Chinese hamster ovary (CHO) cells in a ratio of 1:2 heavy (HC1 and HC2) and light (LC1 and LC2) chains. Charge pair mutations were introduced in the Fc domains: N399K and E356K mutations in the CR6261 heavy-chain Fc domain and K409D and K392D in the 1G01 heavy-chain Fc domain.[29] Seven days following transfection, the supernatant was collected and filtered through a 0.22-mm filter, and the BiAb was purified using protein A affinity column and ultrafiltration. The antibody was also subjected to 0.2-μm sterile filtration and endotoxin removal (<5 EU/mg). Purified proteins were dialyzed in PBS ×1 for overnight and were analyzed by size-exclusion high-performance liquid chromatography (SEC-HPLC) and SDS-PAGE.

Influenza virus infection and flow cytometry

For influenza virus infection, MDCK cells were seeded at 70%–80% confluency and infected with A/Puerto Rico/8/34 (H1N1), A/WS/33 H1N1 (ATCC, VR-219), or A/FM/1/47 H1N1 (ATCC, VR-97) in serum-free DMEM supplemented with trypsin type IX (Sigma, T-0303). The cells were incubated with the virus for 1 h at 37°C, washed with PBS ×1, and incubated for 48 h in complete DMEM supplemented with 4,500 mg/L D-glucose, 4 mM L-glutamine, 110 mg/L sodium pyruvate, 10% FBS, 1% penicillin-streptomycin, and 1% NEAAs. For coating of EL4 cells with A/Puerto Rico/8/34 (H1N1), cells were incubated with the virus for 4 h at 37°C. After the

incubation, staining was performed by harvesting and washing the cells with FACS medium (PBS ×1 supplied with 1% bovine serum albumin). Influenza virus-infected cells were incubated for 1 h at 4°C with primary antibodies CR6261, 1G01, or the BiAb diluted in FACS medium. The cells were then washed with FACS medium and further incubated for 45 min with secondary antibody Alexa Fluor 488-conjugated goat anti-mouse IgG (Jackson, catalog no. 715-545-151, 1:200) and viability dye (Thermo Fisher Scientific, catalog no. 65-0865-14). In experiments where the steric inhibition mediated by CR6261 was tested, 10^5 infected MDCK cells were left untreated or incubated with 1 μg/well of CR6261 for 45 min. The cells were then washed with PBS ×1 and were stained with either 1 μg/well or 5 μg/well of fluorescein isothiocyanate (FITC)-labeled 1G01 (Thermo Fisher Scientific, catalog no. 53027). Staining was evaluated using the BD Biosciences LSRFortessa flow cytometer. Viability dye was used in order to gate on live cells only, and further analysis of the staining results was done using FlowJo software v10.7. For neutralization of A/WS/33 H1N1 or A/FM/1/47 H1N1 in MDCK cells, 1 μg of BiAb was incubated with the virus for 1 h prior to infection. Staining was evaluated 48 h after infection. Staining of uninfected cells with the HA-Ig fusion was done for 1 h at 4°C, followed by staining with anti-human IgG antibody (Jackson, catalog no. 709-136-149) for 30 min at 4°C. The concentrations of the HA-Ig that were used are indicated in the figure. For analyzing lung T cells, lungs were harvested from the infected mice at the indicated time points and were homogenized to a single-cell suspension. The cell suspensions were treated using ammonium chloride (ACK, catalog no. A10492-01) buffer to lyse the red blood cells (RBCs) and followed by repeated washing with complete RPMI1640 medium. The cells were then stained for 45 min at 4°C with mixture of the following antibodies: CD45 (BioLegend, catalog no. 103112), CD3 (BioLegend, catalog no. 100206), CD4 (BioLegend, catalog no. 100567), CD8 (Bio Legend, catalog no. 100725), and CD69 (BioLegend, catalog no. 104505).

For analyzing influenza virus-infected lung epithelial cells in mice, the lungs were harvested from the infected mice at the indicated time points, homogenized to a single-cell suspension, and RBCs were lysed using ammonium chloride (ACK, catalog no. A10492-01) buffer. The cells were then stained primarily with the mixture of the following antibodies for 45 min at 4°C: viability dye (Thermo Fisher Scientific, catalog no. 65-0865-14), CD45 (BioLegend, catalog no. 103112), EpCam (BioLegend, catalog no. 118225), and CR6261 (anti-HA). The cells were then washed with FACS medium and further incubated for 30 min with secondary antibody Alexa Fluor 488-conjugated goat anti-mouse IgG (Jackson, catalog no. 715-545-151, 1:200). Data acquisition for analysis was performed using the BD Biosciences LSRFortessa flow cytometer. Analysis was performed using FlowJo software v10.7.

ELISA

High-protein-binding 96-well plates (Thermo scientific, catalog no. 44-2404-21) were coated with 10 μg/mL of HA or NA glycoproteins or HA and NA together (5 μg/mL) in phosphate-buffered saline (PBS) and kept overnight at 4°C. The next day, the plates were washed twice with washing buffer and blocked for 2 h at room temperature (RT) with a blocking buffer containing PBS ×1 and 2% dry milk. The plates were then incubated with the appropriate primary antibody (CR6261, 1G01, or BiAb) at the concentration of 1 μg/mL for 1.5 h at RT. Next, the plates were washed with wash buffer five or six times and then incubated for 1 h at RT with secondary antibody horseradish peroxidase (HRP)-conjugated goat anti-mouse IgG diluted 1:10,000 (Jackson ImmunoResearch). Finally, the plates were developed by adding 100 μL of HRP substrate TMB Single Solution (Life Technologies, 02049211-7) and the absorbance was measured at 650 nm using a microplate reader (Infinite M200 PRO). The fold change in the optical density (OD) (650 nm) was calculated by dividing each data point with the background OD levels that were measured for each antibody or for the control wells.

Modeling virion-bound antibodies

Several input structures were used in modeling. The virion model, including the membrane, HA, NA, and glycans was obtained from the last frame of all-atom, whole-virion MD simulation of influenza A/45/Michigan/2015 (H1N1).[31,32] Structures of antibodies (Fab fragments) with HA and NA were obtained from the Protein Data Bank (PDB: 4FQV [66] and 6Q1Z [19]). To model the complete IgG, we relied on the IgG structure (PDB: 1IGT).[67] To map all possible antibody interaction sites with the virion, we superimposed the HA-Fab complex on all the HAs of the virion. Similarly, all possible N interaction sites were mapped. Next, we searched for pairs of Fabs (one bound to HA and the other to N) that could be connected via the Fc domain into a complete IgG structure. Due to the flexibility of IgG, especially of the linkers between the Fabs and the Fc domain, we generated 1,000 different conformations of the complete IgG by sampling the linkers between Fabs and Fc.[68] Each antibody conformation was then aligned on each pair of HA and N Fabs in close proximity on the virion surface. We considered the aligned IgG position on top of the virion as valid if the root-mean-square deviation (RMSD) of aligned Fabs was below 10 Å. When multiple IgG conformations could be fitted to the same HA and NA pair, a single one was selected with the lowest RMSD. As a result, 11 IgGs could be placed on top of the virion frame. Furthermore, we replaced the Fabs in each positioned IgG with the experimental structure of the respective HA/NA Fab. All visualizations were done using ChimeraX.[69]

BLI

The BLI assay was performed using an OctetR4 instrument to study the binding affinities between the HA and NA antigens with the BiAb. The assay was initiated by hydrating with the Octet Anti-Penta-HIS (HIS1K) biosensors (Sartorius, catalog no. 18-5120) for 10 min. After hydration, BLI was performed over five steps: initial baseline (60 s), antigen immobilization (300 s), second baseline (120 s), antibody binding (300 s), and dissociation (600 s). Baseline and dissociation steps were performed using the Octet Kinetics Buffer (Sartorius, catalog no. 18–1105). First, HIS1K biosensor surface was loaded for antigen immobilization with the polyhistidine-tagged recombinant HA or NA antigens or HA and NA antigen in combination. This was

followed by the removal of the residual antigen in the second baseline step and loading of the CR6261, 1G01, or BiAb (100 ng) to evaluate the specific interaction between the antigens and antibodies. The antigens were loaded in final (HA + NA) different concentrations as indicated in the figures to examine the effect of the antigen concentration on the association-dissociation pattern. Based on the 1:1 binding model, the binding constants were calculated from the resulting association-dissociation curves. The data were analyzed using the Octet Analysis Studio.

Microneutralization assay

The neutralizing activity of CR6261, 1G01, the BiAb, or a combination of CR6261 and 1G01 were evaluated by microneutralization assays, using a previously described protocol.[33] 1.8×10^3 plaque-forming units (PFU)/mL A/Puerto Rico/8/1934 (H1N1) was incubated with the indicated antibody at various concentrations, starting from 100 μg/mL followed by 1:3 serial dilutions. The mixture was prepared in serum-free DMEM with 1 μg/mL TPCK-treated trypsin (Sigma) and incubated for 1 h at 37°C. The virus was then incubated with MDCK cells seeded in 96-well plates (at 70%–80% confluency) for 1 h at 37°C. Following the incubation, the supernatant was aspirated and replenished with complete DMEM containing the same antibody concentration described above and incubated for 18–22 h at 37°C. The next day, cells were fixed with 100 μL of 80% acetone for 1 h at −20°C, washed, and blocked with blocking buffer (5% non-fat milk diluted in 1× PBS) for 1.5 h at 37°C. The cells were then incubated with 100 μL of biotinylated anti-influenza A nucleoprotein (NP) primary antibody (EMD Millipore) diluted 1:2,000 in blocking buffer. The plates were washed five or six times with wash buffer and incubated with HRP-conjugated streptavidin (Jackson ImmunoResearch) diluted in blocking buffer. Finally, the plates were developed by the addition of the HRP substrate, TMB (Life technologies, catalog no. 002023). The absorbance was immediately measured at 650 nm with an ELISA microplate reader (Infinite M200 PRO). Data were analyzed using GraphPad Prism v8.4 software (GraphPad).

NA inhibition assay

Neutralization of the influenza virus NA by the BiAb was evaluated by the capacity of the BiAb to block the release of progeny viruses from infected MDCK cells. Then 6×10^5 MDCK cells per well were infected with 2.3×10^2 PFU/mL of PR8 and incubated at 37°C for 24 h. The infected cells were then washed with 1× PBS and treated with BiAb or 1G01 or CR6261 antibodies at a concentration of 7.5 μg/mL after being diluted in serum-free DMEM supplemented with 1 μg/mL TPCK-treated trypsin (Sigma). After 1-h incubation at 37°C, the infected cells were washed and incubated with complete DMEM for 48 h at 37°C. The cell supernatants from each well were collected separately and used to infect freshly seeded MDCK cells at a density of 6×10^5 per well. Supernatant from infected cells that were not treated with the antibody was used as a control. Infection was evaluated 48 h later by staining to the HA expression on the surface of infected cells using the CR6261 antibody and calculating the percentage of the live HA^+ cells. Viability dye (Thermo Fisher Scientific, catalog no. 65-0865-14) was used in order to gate on live cells only. Staining was evaluated using the BD LSRFortessa flow cytometer and further analysis was done using FlowJo software v10.7.

MUNANA-based NA inhibition assay

The activity of NA was measured by a fluorescence-based assay using the fluorogenic substrate 4-methylumbelliferyl-*N*-acetylneuraminic acid (MUNANA) (Santa Cruz, sc-251885). MDCK cells were seeded in 96-well plates, infected with 4.6×10^3 PFU/mL of PR8, and were incubated at 37°C. After 24 h, the infected cells were treated with 1 μg/mL of the indicated antibodies, with 10 μg/mL oseltamivir (Tamiflu) or a combination of 1 μg/mL of the indicated antibody (1 μg/mL) and 10 μg/mL oseltamivir. The cells were incubated at RT for 45 min. The MUNANA substrate was diluted to a final concentration of 20 μM in enzyme buffer (32.5 mM 2-(N-morpholino) ethanesulfonic acid [MES)], 4 mM calcium chloride, pH 6.5), which was added to all wells (50 μL/wells) and kept for 1-h incubation at 37°C. After the incubation, the plates were spun down at 1,500 rpm for 3 min. The supernatant was transferred to flat-bottom 96-well black polystyrene plates (Thermo, 7805) and the fluorescence intensity was read immediately by microtiter plate reader (Infinite M200 PRO, Tecan) with excitation and emission filters of 355 and 460 nm, respectively.

CD32a-driven neutrophil activation test

For this, 1.25×10^4 MDCK cells were plated in 96-well flat-bottom plates and infected the next day with influenza PR8 at a multiplicity of infection (MOI) of 0.01. Cells were then incubated for 2 days in DMEM to allow viral spread. Mock-treated uninfected cells were used as control. The day of the assay, MDCK cells were detached by trypsin, transferred into U-bottom 96-well plates, and incubated with the antibodies at indicated concentrations. After 15 min, 2.5×10^4 neutrophils, purified from the bone marrow of $hCD32a^{tg}$ mice lacking all endogenous FcgRs[61] (referred to as hCD32a herein) using the Neutrophil Isolation Kit (Miltenyi Biotec), were added. Plates were spun for 1 min at $300 \times g$ to promote cell contacts and incubated at 37°C for 45 min. Cells were then stained for Ly6G (1A8, BioLegend), CD45 (Rea737, Miltenyi Biotec), CD62L (MEL-14, BD Pharmingen), and CD11b (M1/70 BD Pharmingen) for 30 min at 4°C and fixed with 4% PFA. Data were acquired on an Attune flow cytometer equipped with a Cytkick Max plate reader (Thermo Fisher) and analyzed using FlowJo software. The frequencies of $CD62L^-CD11b^{high}$ cells among $Ly6G^+CD45^+$ cells were determined. The values obtained in the control conditions (neutrophils with antibody but without MDCK cells) were subtracted to calculate antibody-mediated neutrophil activation. Negative values were set to zero.

Jurkat NFAT CD16 reporter assay

CD16 (FcγRIIIa) engagement by the various antibodies was evaluated by using the Jurkat NFAT CD16 reporter cells (InvivoGen, catalog no. jktl-nfat-cd16). First, the expression of CD16 was confirmed by FACS staining using anti-CD16 antibody (BioLegend, catalog no. 980104).

Then, 1×10^5 uninfected and PR8-infected MDCK cells (48 h following infection) were incubated with the CR6261, 1G01, BiAb, or a combination of CR6261 and1G01 for 1 h at 37°C, 5% CO_2. The concentrations of the antibodies are depicted in the figure. The cells were then washed and incubated with 2×10^5 Jurkat NFAT CD16 reporter cells for 6 h at 37°C, 5% CO_2. Next, 25 μL of supernatant was drawn from each well and transferred to an opaque, black, 96-well plate to which 50 μL of QuantiLuc substrate was added, and luminescence was immediately read on a microplate reader (Infinite M200 PRO). The reported values of luminescence that was seen in cells incubated with the infected MDCK cells were normalized to the luminescence in cells that were cultured with uninfected MDCK cells that were incubated with identical concentrations of the antibodies.

Generation of escape mutants against neutralizing antibodies

Escape mutants were generated by serial passage of the virus in increasing amounts of CR6261, 1G01, or BiAb by following a previously described protocol[70] with several modifications. First, 2.3×10^2 PFU/mL of PR8 was incubated with 0.001 μg/μL of CR6261 or 0.002 μg/μL of 1G01 or 0.002 μg/μL of BiAb in serum-free DMEM with 1 μg/mL TPCK-treated trypsin (Sigma) and for 30 min at 37 °C. The viruses were then separately incubated with MDCK cells seeded on a six-well plate after washing with 1× PBS. The plate was kept for 1-h incubation at 37°C with repeated shaking of the plate every 10–15 min. After the incubation, the wells were washed and supplemented with complete DMEM and kept for 48-h incubation at 37°C, 5% CO_2. Then, 48 h following the infection, the infected cells were checked for cytopathic effect (CPE) and the supernatants were collected for further passages in MDCK cells. In the next passage, if the infected cells showed gross 70%–90% CPEs, the antibody concentration was increased 2-fold. However, if CPE was moderate to mild, the antibody concentration was maintained as the previous passage. Moreover, the rate of infections was also evaluated by flow cytometry every 48 h by evaluating the percentage of HA-positive cells. After 10 rounds of passages and similar antibody concentrations between the different groups, supernatants were collected, and viruses were sequenced by SGS for escape mutants.

SGS of viral HA and NA genes

Single-genome amplification and sequencing of influenza A H1N1 virus HA and NA genes was performed for supernatants of infected cells as described previously.[41,71] Viral RNA was isolated from the supernatants using a QIAamp Viral RNA mini kit (Qiagen, catalog no. 52906). cDNA was synthesized using HA-3′-Out primer and SuperScript III Reverse Transcriptase (Invitrogen, catalog no.18080–044). The reaction was performed at 50°C for 1 h followed by an additional 1 h at 55°C and terminated by heat inactivation at 70°C for 15 min and finally treated with RNaseH (Invitrogen, catalog no. EN0201) for 20 min at 37°C. The cDNA was serially diluted and was subjected to two rounds of nested PCR using the out- and in-primer sets of the HA gene. A first round of PCR amplification was performed using out forward ATGAAGGCAAACCTACTGGT and reverse TCAGATGCATATTCTGCACT primers for HA gene, and forward ATGAATCCAAATCAGAAAATAATAA and reverse CTACTTGTCAATGGTGAATGG primers for NA gene. The PCR product from the first round was used as a template for the second round of PCR amplification using in-primer set forward TGTGCACTTGCAGCTG and reverse AACACATCCAGAAACTG ATT for HA gene, and forward AATCTGTCTGGTAGTCGGACT and reverse CTGGCCAAGACCAATCTACAGT primers for NA gene. All PCR reactions were performed using DreamTaq (Thermo Scientific, catalog no. K1082) and were analyzed in 1% agarose gel electrophoresis for the right amplicons. Following the Poisson distribution, the cDNA dilution that yields PCR products in no more than 30% of wells were considered for the generation of libraries. The DNA libraries were prepared by using Illumina Nextera DNA Sample Preparation Kit as previously described.[9,41] Sequencing was performed using the Illumina MiSeq Nano 300 cycle kits and gene alignments were generated using Geneious 9.1.8 (Biomatters). Influenza A virus (A/Puerto Rico/8/1934(H1N1)) (NCBI: 956529) complete genome was used as reference genome. Logo plots were generated using the longitudinal antigenic sequences and sites from intra-host evolution (LASSIE) tool.[54]

Mice infection and antibody administration

Female C57BL/6 mice or BALB/c (6–8 weeks old) were used in all of the *in vivo* experiments, and 4.6×10^3 PFU of PR8 was diluted in PBS ×1 and mice were infected intranasally in a volume of 25 μL. For prophylactic efficacy, first 2 mg/kg or 6 mg/kg of CR6261 antibody were administered i.p. 4 h after infection in order to delineate the dose required for minimal prevention of mouse infection. Accordingly, 2 mg/kg of CR6261, 1G01, a combination of CR6261 + 1G01, or the BiAb antibodies were administered i.p. with 50 μL in each dose. Antibodies were diluted in 1× PBS and were analyzed on SDS-PAGE before injection. Antibodies were injected 4 h before infection. Successful antibody administration was verified by bleeding the mice 3 days following antibody administration and analyzing the antibody levels in ELISA. The mouse weights were monitored daily and recorded for 14 days. For the therapy model, mice were infected with 4.6×10^3 PFU of the indicated H1N1 virus and antibodies were administered i.p. 2 days following the infection (2 mg/kg). Mice that lost more than 25% of their initial weight were scarified. Student's t test and log rank test (for the survival experiments) were used to determine statistically significant differences.

For viral-load measurement, the mouse lungs were harvested 3 or 7 days following infection and the amount of the virus was evaluated by real-time PCR as previously described.[72] Whole-lung tissue was isolated, the weight of the lung samples was measured to ensure an equal sample size, and the lungs were kept at −80°C until further processing. Lungs were homogenized, and 140 μL of the lung sample was used for RNA isolation. Viral RNA was extracted from the lung using a QIAamp RNA extraction kit (Qiagen). The RNA was immediately used for the one-step RT-PCR and qPCR TaqMan reaction using primers for the matrix protein of influenza virus A described by Van Elden et al.[73] For the qPCR, a TaqMan universal PCR master mix containing ROX as a passive reference was used (PE Applied

Biosystems) including 900 nM influenza virus A primers. The qPCR analysis was performed with ABI Prism 7700 sequence detection system. Antibody-treated mice in which no detectable viral loads were seen were excluded from the analysis. In order to generate a standard curve for evaluation of the reaction efficiency and sensitivity, serial dilutions of standard A/Puerto Rico/8/34 (H1N1) RNA were generated (ATCC, VR-95DQ). The resulting Cq values for each RNA concentration were then plotted against the known copies used in each dilution.

To measure the half-life of the BiAb, antibody-treated mice were bled daily after antibody administration. Plasma was then collected and diluted 10-fold in PBS ×1. The levels of the BiAb in the plasma was evaluated by coating an ELISA plate with 0.5 μg of H1N1 HA and H1N1 NA followed by incubation with the diluted plasma samples. Wells were washed and incubated for 1 h at RT with secondary antibody HRP-conjugated goat anti-mouse IgG diluted 1:10,000 (Jackson ImmunoResearch). Plasma from untreated mice was used to calculate the background staining. The levels of the BiAb 3 h after the antibody administration were used to calculate the initial antibody dose in the mice plasma. The antibody $t_{1/2}$ was evaluated by a non-linear regression model using GraphPad Prism v.8.4 software (GraphPad).

Statistical analysis

Statistical significance was calculated by Student's t test and by one- or two-way ANOVA. Statistical differences between survival rates were analyzed by comparing Kaplan-Meier curves using the log rank test. Sample sizes (*n*) for *in vivo* experiments are indicated in the corresponding figures, and the number of biological repeats for experiments and specific tests for statistical significance used are indicated in the corresponding figure legends. Statistical tests that were used to control for multiple comparisons are indicated in the figure legends. Results are presented as mean ± SEM. Data were analyzed using GraphPad Prism v.8.4 software (GraphPad).

DATA AND CODE AVAILABILITY

SGS data are available in GenBank (GenBank: PQ076653-PQ076680, PQ074127-PQ074144, PQ096049-PQ096066, and PQ096443-PQ096463).

SUPPLEMENTAL INFORMATION

Supplemental information can be found online at https://doi.org/10.1016/j.ymthe.2024.07.023.

ACKNOWLEDGMENTS

We are grateful to Lynn E. MacDonald and Andrew L. Murphy, working at Regeneron Pharmaceuticals, for providing MAID 1505 (FcγRIonly) mice used to generate hCD32atg FcγRnull mice. We thank the Technion genome facility for their assistance with the SGS analysis. We acknowledge the staff of the biomedical core facility (Faculty of Medicine, Technion) for their help with the flowcytometry experiments. We thank Sartorius Israel Ltd. for their help with the BLI analysis and Creative Biolabs for facilitating the antibody purifications. Illustrations were generated using BioRender. We thank Shubham B. Deshmukh for his help with the protein analysis. This study was funded by the following research grants: The Israeli Ministry of Science and Technology MOST: France-Israel Joint Projects (0005201) to Y.B.-O. and T.B., The Israel Science Foundation, Israel-Canada Collaboration (2071058) to Y.B.-O., The–US Israel Binational Science Foundation (BSF, 2021068) to Y.B.-O., The Rapoport Faculty of Medicine SPARK grant to Y.B.-O., and The Michigan-Israel Partnership to Y.B.-O.

AUTHOR CONTRIBUTIONS

R.M. designed and conducted experiments, analyzed data, and wrote the paper. S.C. and D.K. conducted experiments. B.S., D.S.-D., M.M., F.J., T.B., I.K., and J.W.Y. contributed to the design of the experimental strategy. Y.B.-O. supervised the study, designed the experiments, wrote the paper, and acquired funding.

DECLARATION OF INTERESTS

A provisional patent on BiAb is currently being filed, in which Y.B.-O. and R.M. are inventors.

REFERENCES

1. Crowe, J.E. (2018). Is it possible to develop a "universal" influenza virus vaccine?: Potential for a universal influenza vaccine. Cold Spring Harbor Perspect. Biol. *10*, a029496. https://doi.org/10.1101/cshperspect.a029496.

2. Nypaver, C., Dehlinger, C., and Carter, C. (2021). Influenza and Influenza Vaccine: A Review. J. Midwifery Womens Health *66*, 45–53. https://doi.org/10.1111/jmwh.13203.

3. Freund, N.T., Wang, H., Scharf, L., Nogueira, L., Horwitz, J.A., Bar-On, Y., Golijanin, J., Sievers, S.A., Sok, D., Cai, H., et al. (2017). Coexistence of potent HIV-1 broadly neutralizing antibodies and antibody-sensitive viruses in a viremic controller. Sci. Transl. Med. *9*, eaal2144. https://doi.org/10.1126/scitranslmed.aal2144.

4. Naranjo-Gomez, M., and Pelegrin, M. (2019). Vaccinal effect of HIV-1 antibody therapy. Curr. Opin. HIV AIDS *14*, 325–333. https://doi.org/10.1097/COH.0000000000000555.

5. Caskey, M., Schoofs, T., Gruell, H., Settler, A., Karagounis, T., Kreider, E.F., Murrell, B., Pfeifer, N., Nogueira, L., Oliveira, T.Y., et al. (2017). Antibody 10-1074 suppresses viremia in HIV-1-infected individuals. Nat. Med. *23*, 185–191. https://doi.org/10.1038/nm.4268.

6. Caskey, M., Klein, F., Lorenzi, J.C.C., Seaman, M.S., West, A.P., Buckley, N., Kremer, G., Nogueira, L., Braunschweig, M., Scheid, J.F., et al. (2015). Viraemia suppressed in HIV-1-infected humans by broadly neutralizing antibody 3BNC117. Nature *522*, 487–491. https://doi.org/10.1038/nature14411.

7. Chai, N., Swem, L.R., Reichelt, M., Chen-Harris, H., Luis, E., Park, S., Fouts, A., Lupardus, P., Wu, T.D., Li, O., et al. (2016). Two Escape Mechanisms of Influenza A Virus to a Broadly Neutralizing Stalk-Binding Antibody. Plos Pathog. *12*, e1005702. https://doi.org/10.1371/journal.ppat.1005702.

8. Prachanronarong, K.L., Canale, A.S., Liu, P., Somasundaran, M., Hou, S., Poh, Y.-P., Han, T., Zhu, Q., Renzette, N., Zeldovich, K.B., et al. (2019). Mutations in Influenza A Virus Neuraminidase and Hemagglutinin Confer Resistance against a Broadly Neutralizing Hemagglutinin Stem Antibody. J. Virol. *93*, e01639-17. https://doi.org/10.1128/jvi.01639-18.

9. Bar-On, Y., Gruell, H., Schoofs, T., Pai, J.A., Nogueira, L., Butler, A.L., Millard, K., Lehmann, C., Suárez, I., Oliveira, T.Y., et al. (2018). Safety and antiviral activity of combination HIV-1 broadly neutralizing antibodies in viremic individuals. Nat. Med. *24*, 1701–1707. https://doi.org/10.1038/s41591-018-0186-4.

10. Abraham, J. (2020). Passive antibody therapy in COVID-19. Nat. Rev. Immunol. *20*, 401–403. https://doi.org/10.1038/s41577-020-0365-7.

11. Scott, A.M., Wolchok, J.D., and Old, L.J. (2012). Antibody therapy of cancer. Nat. Rev. Cancer *12*, 278–287. https://doi.org/10.1038/nrc3236.

12. Biswas, M., Yamazaki, T., Chiba, J., and Akashi-Takamura, S. (2020). Broadly neutralizing antibodies for influenza: Passive immunotherapy and intranasal vaccination. Vaccines (Basel) *8*, 424. https://doi.org/10.3390/vaccines8030424.

13. Laursen, N.S., and Wilson, I.A. (2013). Broadly neutralizing antibodies against influenza viruses. Antivir. Res. *98*, 476–483. https://doi.org/10.1016/j.antiviral.2013.03.021.

14. Dou, D., Revol, R., Östbye, H., Wang, H., and Daniels, R. (2018). Influenza A virus cell entry, replication, virion assembly and movement. Front. Immunol. *9*, 1581. https://doi.org/10.3389/fimmu.2018.01581.

15. Kirkpatrick, E., Qiu, X., Wilson, P.C., Bahl, J., and Krammer, F. (2018). The influenza virus hemagglutinin head evolves faster than the stalk domain. Sci. Rep. *8*, 10432. https://doi.org/10.1038/s41598-018-28706-1.

16. Crowe, J.E. (2012). Influenza virus resistance to human neutralizing antibodies. mBio *3*, e00213. https://doi.org/10.1128/mBio.00213-12.

17. Doud, M.B., Lee, J.M., and Bloom, J.D. (2018). How single mutations affect viral escape from broad and narrow antibodies to H1 influenza hemagglutinin. Nat. Commun. *9*, 1386. https://doi.org/10.1038/s41467-018-03665-3.

18. Park, J.K., Xiao, Y., Ramuta, M.D., Rosas, L.A., Fong, S., Matthews, A.M., Freeman, A.D., Gouzoulis, M.A., Batchenkova, N.A., Yang, X., et al. (2020). Pre-existing immunity to influenza virus hemagglutinin stalk might drive selection for antibody-escape mutant viruses in a human challenge model. Nat. Med. *26*, 1240–1246. https://doi.org/10.1038/s41591-020-0937-x.

19. Stadlbauer, D., Zhu, X., McMahon, M., Turner, J.S., Wohlbold, T.J., Schmitz, A.J., Strohmeier, S., Yu, W., Nachbagauer, R., Mudd, P.A., et al. (2019). Broadly protective human antibodies that target the active site of influenza virus neuraminidase. Science *366*, 499–504. https://doi.org/10.1126/science.aay0678.

20. McAuley, J.L., Gilbertson, B.P., Trifkovic, S., Brown, L.E., and McKimm-Breschkin, J.L. (2019). Influenza virus neuraminidase structure and functions. Front. Microbiol. *10*, 39. https://doi.org/10.3389/fmicb.2019.00039.

21. Gaymard, A., Le Briand, N., Frobert, E., Lina, B., and Escuret, V. (2016). Functional balance between neuraminidase and haemagglutinin in influenza viruses. Clin. Microbiol. Infect. *22*, 975–983. https://doi.org/10.1016/j.cmi.2016.07.007.

22. Wagner, R., Matrosovich, M., and Klenk, H.D. (2002). Functional balance between haemagglutinin and neuraminidase in influenza virus infections. Rev. Med. Virol. *12*, 159–166. https://doi.org/10.1002/rmv.352.

23. Kosik, I., and Yewdell, J.W. (2019). Influenza hemagglutinin and neuraminidase: Yin–yang proteins coevolving to thwart immunity. Viruses *11*, 346. https://doi.org/10.3390/v11040346.

24. Kosik, I., Angeletti, D., Gibbs, J.S., Angel, M., Takeda, K., Kosikova, M., Nair, V., Hickman, H.D., Xie, H., Brooke, C.B., and Yewdell, J.W. (2019). Neuraminidase inhibition contributes to influenza A virus neutralization by anti-hemagglutinin stem antibodies. J. Exp. Med. *216*, 304–316. https://doi.org/10.1084/jem.20181624.

25. Marathe, B.M., Arunkumar, G.A., Vogel, P., Pascua, P.N.Q., Jones, J., Webby, R.J., Krammer, F., and Govorkova, E.A. (2020). Monoclonal antibody therapy protects pharmacologically immunosuppressed mice from lethal infection with influenza B virus. Antimicrob. Agents Chemother. *64*, e00284-20. https://doi.org/10.1128/AAC.00284-20.

26. Hehle, V., Beretta, M., Bourgine, M., Ait-Goughoulte, M., Planchais, C., Morisse, S., Vesin, B., Lorin, V., Hieu, T., Stauffer, A., et al. (2020). Potent human broadly neutralizing antibodies to hepatitis B virus from natural controllers. J. Exp. Med. *217*, e20200840. https://doi.org/10.1084/JEM.20200840.

27. Ekiert, D.C., Bhabha, G., Elsliger, M., Friesen, R.H.E., Jongeneelen, M., Throsby, M., Goudsmit, J., and Wilson, I.A. (2009). Antibody recognition of a highly conserved influenza virus epitope : implications for universal prevention and therapy. Science *324*, 246–251.

28. Ekiert, D.C., and Wilson, I.A. (2012). Broadly neutralizing antibodies against influenza virus and prospects for universal therapies. Curr. Opin. Virol. *2*, 134–141. https://doi.org/10.1016/j.coviro.2012.02.005.

29. Gunasekaran, K., Pentony, M., Shen, M., Garrett, L., Forte, C., Woodward, A., Ng, S.B., Born, T., Retter, M., Manchulenko, K., et al. (2010). Enhancing antibody Fc heterodimer formation through electrostatic steering effects: Applications to bispecific molecules and monovalent IgG. J. Biol. Chem. *285*, 19637–19646. https://doi.org/10.1074/jbc.M110.117382.

30. Bar-On, Y., Glasner, A., Meningher, T., Achdout, H., Gur, C., Lankry, D., Vitenshtein, A., Meyers, A.F.A., Mandelboim, M., and Mandelboim, O. (2013). Neuraminidase-Mediated, NKp46-Dependent Immune-Evasion Mechanism of Influenza Viruses. Cell Rep. *3*, 1044–1050. https://doi.org/10.1016/j.celrep.2013.03.034.

31. Casalino, L., Seitz, C., Lederhofer, J., Tsybovsky, Y., Wilson, I.A., Kanekiyo, M., and Amaro, R.E. (2022). Breathing and Tilting: Mesoscale Simulations Illuminate Influenza Glycoprotein Vulnerabilities. ACS Cent. Sci. *8*, 1646–1663. https://doi.org/10.1021/acscentsci.2c00981.

32. Durrant, J.D., Kochanek, S.E., Casalino, L., Ieong, P.U., Dommer, A.C., and Amaro, R.E. (2020). Mesoscale All-Atom Influenza Virus Simulations Suggest New Substrate Binding Mechanism. ACS Cent. Sci. *6*, 189–196. https://doi.org/10.1021/acscentsci.9b01071.

33. Bournazos, S., Corti, D., Virgin, H.W., and Ravetch, J.V. (2020). Fc-optimized antibodies elicit CD8 immunity to viral respiratory infection. Nature *588*, 485–490. https://doi.org/10.1038/s41586-020-2838-z.

34. Karthick, V., Shanthi, V., Rajasekaran, R., and Ramanathan, K. (2013). In silico analysis of drug-resistant mutant of neuraminidase (N294S) against oseltamivir. Protoplasma *250*, 197–207. https://doi.org/10.1007/s00709-012-0394-6.

35. Yasuhara, A., Yamayoshi, S., Kiso, M., Sakai-Tagawa, Y., Okuda, M., and Kawaoka, Y. (2022). A broadly protective human monoclonal antibody targeting the sialidase activity of influenza A and B virus neuraminidases. Nat. Commun. *13*, 6602. https://doi.org/10.1038/s41467-022-34521-0.

36. Chen, Y.-Q., Lan, L.Y.-L., Huang, M., Henry, C., and Wilson, P.C. (2019). Hemagglutinin Stalk-Reactive Antibodies Interfere with Influenza Virus Neuraminidase Activity by Steric Hindrance. J. Virol. *93*, e01526-18. https://doi.org/10.1128/jvi.01526-18.

37. Cagle, L.A., Linderholm, A.L., Franzi, L.M., Last, J.A., Simon, S.I., Kenyon, N.J., and Harper, R.W. (2022). Early mechanisms of neutrophil activation and transmigration in acute lung injury. Front. Physiol. *13*, 1059686. https://doi.org/10.3389/fphys.2022.1059686.

38. Schultz-Cherry, S. (2015). Role of nk cells in influenza infection. Curr. Top. Microbiol. Immunol. *386*, 109–120. https://doi.org/10.1007/82_2014_403.

39. van der Pol, W., and van de Winkel, J.G. (1998). IgG receptor polymorphisms: Risk factors for disease. Immunogenetics *48*, 222–232. https://doi.org/10.1007/s002510050426.

40. Carrat, F., and Flahault, A. (2007). Influenza vaccine: The challenge of antigenic drift. Vaccine *25*, 6852–6862. https://doi.org/10.1016/j.vaccine.2007.07.027.

41. Horwitz, J.A., Bar-On, Y., Lu, C.L., Fera, D., Lockhart, A.A.K., Lorenzi, J.C.C., Nogueira, L., Golijanin, J., Scheid, J.F., Seaman, M.S., et al. (2017). Non-neutralizing Antibodies Alter the Course of HIV-1 Infection *In Vivo*. Cell *170*, 637–648.e10. https://doi.org/10.1016/j.cell.2017.06.048.

42. Wu, N.C., and Wilson, I.A. (2020). Influenza hemagglutinin structures and antibody recognition. Cold Spring Harbor Perspect. Med. *10*, a038778. https://doi.org/10.1101/cshperspect.a038778.

43. Gamblin, S.J., Vachieri, S.G., Xiong, X., Zhang, J., Martin, S.R., and Skehel, J.J. (2021). Hemagglutinin structure and activities. Cold Spring Harbor Perspect. Med. *11*, a038638. https://doi.org/10.1101/cshperspect.a038638.

44. Throsby, M., van den Brink, E., Jongeneelen, M., Poon, L.L.M., Alard, P., Cornelissen, L., Bakker, A., Cox, F., van Deventer, E., Guan, Y., et al. (2008). Heterosubtypic neutralizing monoclonal antibodies cross-protective against H5N1 and H1N1 recovered from human IgM+ memory B cells. PLoS One *3*, e3942. https://doi.org/10.1371/journal.pone.0003942.

45. Pavia, C.S., and Wormser, G.P. (2021). Passive immunization and its rebirth in the era of the COVID-19 pandemic. Int. J. Antimicrob. Agents *57*, 106275. https://doi.org/10.1016/j.ijantimicag.2020.106275.

46. Yang, J., Liu, S., Du, L., and Jiang, S. (2016). A new role of neuraminidase (NA) in the influenza virus life cycle: implication for developing NA inhibitors with novel mechanism of action. Rev. Med. Virol. *26*, 242–250. https://doi.org/10.1002/rmv.1879.

47. Ellis, D., Lederhofer, J., Acton, O.J., Tsybovsky, Y., Kephart, S., Yap, C., Gillespie, R.A., Creanga, A., Olshefsky, A., Stephens, T., et al. (2022). Structure-based design of stabilized recombinant influenza neuraminidase tetramers. Nat. Commun. *13*, 1825. https://doi.org/10.1038/s41467-022-29416-z.

48. Samji, T. (2009). Influenza A: Understanding the viral life cycle. Yale J. Biol. Med. *82*, 153–159.

49. Matrosovich, M.N., Matrosovich, T.Y., Gray, T., Roberts, N.A., and Klenk, H.-D. (2004). Neuraminidase Is Important for the Initiation of Influenza Virus Infection in Human Airway Epithelium. J. Virol. *78*, 12665–12667. https://doi.org/10.1128/jvi.78.22.12665-12667.2004.

50. Eichelberger, M.C., and Monto, A.S. (2019). Neuraminidase, the Forgotten Surface Antigen, Emerges as an Influenza Vaccine Target for Broadened Protection. J. Infect. Dis. *219*, S75–S80. https://doi.org/10.1093/infdis/jiz017.

51. Zanin, M., Duan, S., Wong, S.-S., Kumar, G., Baviskar, P., Collin, E., Russell, C., Barman, S., Hause, B., and Webby, R. (2017). An Amino Acid in the Stalk Domain of N1 Neuraminidase Is Critical for Enzymatic Activity. J. Virol. *91*, e00868-16. https://doi.org/10.1128/jvi.00868-16.

52. DiLillo, D.J., and Ravetch, J.V. (2015). Differential Fc-receptor engagement drives an anti-tumor vaccinal effect. Cell *161*, 1035–1045. https://doi.org/10.1016/j.cell.2015.04.016.

53. Nishimura, Y., Gautam, R., Chun, T.W., Sadjadpour, R., Foulds, K.E., Shingai, M., Klein, F., Gazumyan, A., Golijanin, J., Donaldson, M., et al. (2017). Early antibody therapy can induce long-lasting immunity to SHIV. Nature *543*, 559–563. https://doi.org/10.1038/nature21435.

54. Schoofs, T., Klein, F., Braunschweig, M., Kreider, E.F., Feldmann, A., Nogueira, L., Oliveira, T., Lorenzi, J.C.C., Parrish, E.H., Learn, G.H., et al. (2016). HIV-1 therapy with monoclonal antibody 3BNC117 elicits host immune responses against HIV-1. Science *352*, 997–1001. https://doi.org/10.1126/science.aaf0972.

55. Yuen, G., Bhanot, S., Steen, J., Syed, M., and Mardon, A. (2020). Bispecific Antibodies as an Alternative to Antibody Cocktails for SARS-CoV-2: A Mini- Review. J. Immunol. Sci. *6*, 18–24. https://doi.org/10.29245/2578-3009/2022/2.1237.

56. Metzger, L. (2022). REGEN-COV Antibody Combination and Outcomes in Outpatients with Covid-19. Pneumologie *76*, e81. https://doi.org/10.1055/a-1697-9788.

57. F, W., J, M., J, M., N, M., A, E., and J, B. (2023). Effectiveness of REGEN-COV antibody combination to reduce risk of hospitalization for pregnant patients with COVID-19. Am. J. Obstet. Gynecol. *228*, S791–S792. https://doi.org/10.1016/j.ajog.2022.11.157.

58. Bassetti, M., Castaldo, N., and Carnelutti, A. (2019). Neuraminidase inhibitors as a strategy for influenza treatment: pros, cons and future perspectives. Expert Opin. Pharmacother. *20*, 1711–1718. https://doi.org/10.1080/14656566.2019.1626824.

59. Cheng, W., Pan, A., Rathbun, S.L., Ge, Y., Xiao, Q., Martinez, L., Ling, F., Liu, S., Wang, X., Yu, Z., et al. (2021). Effectiveness of neuraminidase inhibitors to prevent mortality in patients with laboratory-confirmed avian influenza A H7N9. Int. J. Infect. Dis. *103*, 573–578. https://doi.org/10.1016/j.ijid.2020.12.028.

60. Laborda, P., Wang, S.Y., and Voglmeir, J. (2016). Influenza neuraminidase inhibitors: Synthetic approaches, derivatives and biological activity. Molecules *21*, 1513. https://doi.org/10.3390/molecules21111513.

61. Beutier, H., Hechler, B., Godon, O., Wang, Y., Gillis, C.M., De Chaisemartin, L., Gouel-Chéron, A., Magnenat, S., Macdonald, L.E., Murphy, A.J., et al. (2018). Platelets expressing IgG receptor FcγRIIA/CD32A determine the severity of experimental anaphylaxis. Sci. Immunol. *3*, eaan5997. https://doi.org/10.1126/sciimmunol.aan5997.

62. Bar-On, Y., Seidel, E., Tsukerman, P., Mandelboim, M., and Mandelboim, O. (2014). Influenza virus uses its neuraminidase protein to evade the recognition of two activating NK cell receptors. J. Infect. Dis. *210*, 410–418. https://doi.org/10.1093/infdis/jiu094.

63. Tzeng, T.T., Chen, P.L., Weng, T.C., Tsai, S.Y., Lai, C.C., Chou, H.I., Chen, P.W., Lu, C.C., Liu, M.T., Sung, W.C., et al. (2020). Development of high-growth influenza H7N9 prepandemic candidate vaccine viruses in suspension MDCK cells. J. Biomed. Sci. *27*, 47. https://doi.org/10.1186/s12929-020-00645-y.

64. Tiller, T., Meffre, E., Yurasov, S., Tsuiji, M., Nussenzweig, M.C., and Wardemann, H. (2008). Efficient generation of monoclonal antibodies from single human B cells by single cell RT-PCR and expression vector cloning. J. Immunol. Methods *329*, 112–124. https://doi.org/10.1016/j.jim.2007.09.017.

65. Bar-On, Y., Charpak-Amikam, Y., Glasner, A., Isaacson, B., Duev-Cohen, A., Tsukerman, P., Varvak, A., Mandelboim, M., and Mandelboim, O. (2017). NKp46 Recognizes the Sigma1 Protein of Reovirus: Implications for Reovirus-Based Cancer Therapy. J. Virol. *91*, e01045-17. https://doi.org/10.1128/jvi.01045-17.

66. Dreyfus, C., Laursen, N.S., Kwaks, T., Zuijdgeest, D., Khayat, R., Ekiert, D.C., Lee, J.H., Metlagel, Z., Bujny, M.V., Jongeneelen, M., et al. (2012). Highly conserved protective epitopes on influenza B viruses. Science *337*, 1343–1348. https://doi.org/10.1126/science.1222908.

67. Harris, L.J., Larson, S.B., Hasel, K.W., and McPherson, A. (1997). Refined structure of an intact IgG2a monoclonal antibody. Biochemistry *36*, 1581–1597. https://doi.org/10.1021/bi962514+.

68. Chen, Q., Vieth, M., Timm, D.E., Humblet, C., Schneidman-Duhovny, D., Chemmama, I.E., Sali, A., Zeng, W., Lu, J., and Liu, L. (2017). Reconstruction of 3D structures of MET antibodies from electron microscopy 2D class averages. PLoS One *12*, e0175758. https://doi.org/10.1371/journal.pone.0175758.

69. Pettersen, E.F., Goddard, T.D., Huang, C.C., Meng, E.C., Couch, G.S., Croll, T.I., Morris, J.H., and Ferrin, T.E. (2021). UCSF ChimeraX: Structure visualization for researchers, educators, and developers. Protein Sci. *30*, 70–82. https://doi.org/10.1002/pro.3943.

70. Ilyushina, N.A., Lee, N., Lugovtsev, V.Y., Kan, A., Bovin, N.V., and Donnelly, R.P. (2020). Adaptation of influenza B virus by serial passage in human airway epithelial cells. Virology *549*, 68–76. https://doi.org/10.1016/j.virol.2020.08.004.

71. Khateeb, D., Gabrieli, T., Sofer, B., Hattar, A., Cordela, S., Chaouat, A., Spivak, I., Lejbkowicz, I., Almog, R., Mandelboim, M., and Bar-On, Y. (2022). SARS-CoV-2 variants with reduced infectivity and varied sensitivity to the BNT162b2 vaccine are developed during the course of infection. Plos Pathog. *18*, e1010242. https://doi.org/10.1371/journal.ppat.1010242.

72. Hindiyeh, M., Levy, V., Azar, R., Varsano, N., Regev, L., Shalev, Y., Grossman, Z., and Mendelson, E. (2005). Evaluation of a multiplex real-time reverse transcriptase PCR assay for detection and differentiation of influenza viruses A and B during the 2001-2002 influenza season in Israel. J. Clin. Microbiol. *43*, 589–595. https://doi.org/10.1128/JCM.43.2.589-595.2005.

73. van Elden, L.J., Nijhuis, M., Schipper, P., Schuurman, R., and Van Loon, A.M. (2001). Simultaneous detection of influenza viruses A and B using real-time quantitative PCR. J. Clin. Microbiol. *39*, 196–200. https://doi.org/10.1128/JCM.39.1.196-200.2001.